INSTITUTO POTOSINO DE INVESTIGACIÓN CIENTÍFICA Y TECNOLÓGICA, A.C.

POSGRADO EN CIENCIAS EN BIOLOGÍA MOLECULAR

Identification and characterization of contemporaneous clinical isolates of *Candida glabrata*

Tesis que presenta

Oscar Daniel Aranda Moreno

Para obtener el grado de

Maestro en Ciencias en Biología Molecular

Codirectores de la Tesis:

Dra. Irene Beatriz Castaño Navarro

Dr. Marco Josué Hernández Chávez

San Luis Potosí, S.L.P., junio de 2025

Constancia de aprobación de la tesis

La tesis "**Identification and characterization of contemporaneous clinical isolates of *Candida glabrata***" presentada para obtener el grado de Maestro en Ciencias en Biología Molecular fue elaborada por **Oscar Daniel Aranda Moreno** y aprobada el 9 de junio de 2025 por los suscritos, designados por el Colegio de Profesores de la División de Biología Molecular del Instituto Potosino de Investigación Científica y Tecnológica, A.C

_____

Dra. Irene Beatriz Castaño Navarro
Codirectora de la tesis

_____

Dr. Marco Josué Hernández Chávez
Codirector de la tesis

_____

Dr. J. Sergio Casas Flores
Miembro del Comité Tutoral

Créditos institucionales

Esta tesis fue elaborada en el Laboratorio de Microbiología Molecular de la División de Biología Molecular del Instituto Potosino de Investigación Científica y Tecnológica, A.C., bajo la codirección de la Dra. Irene Beatriz Castaño Navarro y el Dr. Marco Josué Hernández Chávez.

Durante la realización del trabajo el autor recibió una beca académica del Consejo Nacional de Ciencia y Tecnología (No. 1309953) y del Instituto Potosino de Investigación Científica y Tecnológica, A. C.

Este trabajo fue apoyado por el proyecto No. 2024-03-M28 del Fondo: Multas Electorales Convocatoria 2024-03. Proyectos de Investigación, Desarrollo e Innovación, otorgado a Irene Beatriz Castaño Navarro

Durante el desarrollo de esta tesis tuvimos el apoyo del Laboratorio Nacional de Biotecnología Agrícola, Médica y Ambiental (LANBAMA), así como del Laboratorio de Microscopía para Muestras Biológicas de la División de Biología Molecular del IPICYT

Dedicatorias

A mi mamá, por su apoyo incondicional y siempre creer en mí. Por estar conmigo en todo momento y por sus consejos valiosos que me han ayudado a superar diferentes obstáculos.

A mi hermano, por siempre sacarme una sonrisa en momentos de estrés. Por ser mi amigo en la vida y apoyarme en cada momento.

A mi papá, por estar para mí siempre, por brindarme sus consejos y sabiduría.

A mi tía Chayo y mis primos Koyin, Deysi, Lupita, Aide y Thanya, por ser un apoyo incondicional, no solo para mí, sino para mi familia, en todo aspecto.

A Mia, Smolov, Cherisev y Lola, por hacerme feliz desde que llegaron a mi vida.

Agradecimientos

Al Instituto Potosino de Investigación Científica y Tecnológica A.C. por el apoyo institucional.

Al Consejo Nacional de Humanidades, Ciencias y Tecnología por la beca otorgada para la realización de mis estudios de maestría.

A la Dra. Irene Castaño por todo el apoyo, consejos, paciencia, guía y enseñanza tanto académicas como durante mi trabajo de tesis, además de su calidez desde que llegue al laboratorio.

Al Dr. Marco Hernández Chávez por ser un gran guía durante mi trabajo, por su gran paciencia, consejos, ideas y aportaciones y especialmente, por nunca dejarme solo y siempre estar al pendiente cuando tenía dificultades.

A la Dra. Guadalupe Gutiérrez Escobedo, por sus excelentes enseñanzas y aportaciones y el apoyo técnico en los diferentes experimentos.

A Gloria López por siempre invaluable labor en el laboratorio para que unca falte material, ya que, sin su ayuda, el avance el proyecto no hubiese sido posible.

A la Dra. Olga Araceli Patrón por su colaboración para obtener imágenes de microcopia de fluorescencia.

Al Dr. Saúl Jijón y al Dr. Nicolás Gómez por el apoyo técnico brindado y el espacio para el uso de equipo de laboratorio.

Al LANBAMA, por su apoyo, colaboración y recursos brindados para la realización del proyecto.

A mis amigos de la maestría Daniel, Mario, Fausto, Armando y Alberto, porque sin sus palabras de aliento, consejos, conocimientos y risas, este camino hubiese sido muy difícil.

A mis compañeros y amigos del Laboratorio 6, por recibirme con los brazos abiertos y siempre tener una sonrisa para cada situación, por su apoyo, consejos y risas. Y a Mariana, Belén, Grecia, Antonio y Alex que se volvieron especiales durante el transcurso de mi maestría y nunca me dejaron caer en el laboratorio.

Contenido

Lista de tablas

Lista de figuras

Anexos

Abreviaturas

CAA - Casaminoacids

CSP - Caspofungin

CSP^R - Caspofungin resistant

CSP^S - Caspofungin sensitive

FLC - Fluconazole

FLC^R - Fluconazole resistant

FLC^S - Fluconazole sensitive

GOF - Gain of Function

H_2O_2 - Hydrogen Peroxide

IAH - Independent Action Hypothesis

MLP - Microsatellite Length Polymorphism

NCV - Normal Colony Variant

OD_{600} - Optical Density

P – Patient followed by the corresponding number

RAPD - Random Amplification Polymorphic DNA

SCV - Small Colony Variant

WHO - World Health Organization

YPD - Yeast Extract Peptone Dextrose

YPG - Yeast Extract Peptone Glycerol

Resumen

Identificación y caracterización de aislados clínicos contemporáneos de *Candida glabrata*

El diagnóstico preciso de infecciones sistémicas causadas por patógenos oportunistas como *Candida glabrata*, es necesario para ofrecer una terapia apropiada al paciente. Actualmente, los técnicos de laboratorio clínico diagnostican a *Candida glabrata*, y otros patógenos, mediante la identificación y la caracterización de una única colonia proveniente de muestras clínicas (cepa índice) al inicio y durante el transcurso de la infección (cepas longitudinales), para detectar resistencia a antifúngicos. Esta metodología está basada en la **H**ipótesis de **A**cción **I**ndependiente (HAI) que establece que uno o varios individuos de una población homogénea infecciosa, genotípica y fenotípicamente idéntica es responsable de causar una infección. En este estudio, identificamos 77 aislados clínicos contemporáneos de *C. glabrata* (múltiples cepas índice obtenidas de muestras clínicas únicas de sangre u orina en un punto de infección) de 11 pacientes utilizando PCR con oligonucleótidos especie-específicos. Además, genotipificamos las cepas utilizando marcadores moleculares (*RPM2*, *MT-I*, *ERG3, EPA1* y método RAPD) y determinamos que las cepas comparten un origen clonal por paciente. Además, caracterizamos la respuesta de las cepas contemporáneas en diferentes estreses mediante un ensayo de crecimiento en gota, donde los aislados de los pacientes P6, P17 y P18 mostraron variabilidad fenotípica. La tinción mitocondrial realizada a cuatro cepas “petites” provenientes del P17, mostró una señal difusa en el interior de la célula, diferente a las cepas Gly+ con *foci* localizados y redes mitocondriales. Finalmente, secuenciamos el gen *PDR1* de dos cepas resistentes a FLC e identificamos dos mutaciones (S76P y T143P), que, sin embargo, no están relacionadas con la resistencia a FLC. Este estudio demuestra que, hay variabilidad fenotípica no solo en cepas longitudinales, sino también en cepas contemporáneas.

PALABRAS CLAVE**.** HAI, cepas longitudinales, cepas contemporáneas, infección, variabilidad y resistencia a antifúngicos.

Abstract

Identification and characterization of contemporaneous clinical isolates of *Candida glabrata*

Accurate diagnosis of systemic infections caused by opportunistic pathogens, such as Candida glabrata, is necessary to provide an appropriate therapy to the patient. Currently, clinical laboratory technicians diagnose *C. glabrata* and other pathogens by identifying and characterizing a single colony from clinical samples (index strain). During the infection, they also characterize longitudinal strains to detect fungal resistance. This methodology is based on the **I**ndependent **A**ction **H**ypothesis (IAH), which assumes that one or several individuals from a homogenous infectious population that is genotypically and phenotypically identical is responsible for the infection. In this study, we identified 77 contemporaneous clinical isolates of *C. glabrata* consisting of multiple index strains obtained from single blood or urine clinical samples at a specific time point during the infection. The clinical samples were obtained from 11 patients and identified by PCR using species-specific primers. We then genotyped them using four molecular markers (MLP: *RPM2*, *MT-I*, *ERG3*, and *EPA1* genes), suggesting that isolates from each patient share a clonal origin. We also characterized the response of the contemporaneous strains to several different stresses by drop-spot assay and found phenotypic variability among contemporaneous strains from patients P6 (blood), P17 (urine), and P18 (urine). In addition, we stained the mitochondria in four petite strains (Gly-) derived from P17, which showed a diffuse signal within the cell, unlike the localized foci and mitochondrial network in the Gly+ strains. Finally, we sequenced the *PDR1* gene from two FLC^R strains and identified two mutations (S76P and T143P). However, these SNPs are unrelated to antifungal resistance. These data show that phenotypic variability is present not only in longitudinal strains but also in contemporaneous strains, which can lead to treatment failure.

KEY WORDS**.** IAH, longitudinal strains, contemporaneous strains, Infection, variability, antifungal resistance.

Introduction

Infections caused by fungal pathogens are important to public health because of the high morbidity and mortality rates associated with them. An accurate diagnosis can offer appropriate therapy and a better patient prognosis (1,2). Identifying and characterizing etiological agents are crucial in all infection cases because each pathogen has different antifungal susceptibility profiles. However, the proper diagnosis and characterization of some of these pathogens are challenging due to a lack of rapid, accurate, and sensitive methods to diagnose candidemia. On the other hand, the high capability of the pathogen to grow, multiply, and adapt to its host can lead to the acquisition of mutations that can confer resistance to antibiotics or antifungals, resulting in a persistent infection. (1,3,4).

Among these pathogens, we find *Candida* spp., which form part of the human microbiome and can colonize different anatomical sites, especially mucosal surfaces. However, a small portion of *Candida* spp. are opportunistic fungal pathogens capable of causing invasive infections in immunocompromised patients (5,6). According to the World Health Organization (WHO), there are six priority *Candida* spp.: *Candida albicans*, *Candida glabrata*, *Candida tropicalis*, *Candida parapsilosis*, *Candida krusei*, and *Candida auris* (7). *C. glabrata* leads the high-priority group because it is the second most common species responsible for systemic candidiasis worldwide after *Candida albicans* and it is associated with high mortality rates because it displays multiple virulence factors that are crucial throughout the infection (8–10) such as innate and acquired resistance to azoles and echinocandins, the two main classes of antifungals to treat candidiasis, high adherence to tissues and medical devices, high resistance to oxidative stress and heat shock, and a considerable genomic plasticity (11).

Currently, diagnosis of *C. glabrata* and other pathogens is based on the identification and characterization of a single colony (index strain) from the initial sample, and during the infection (days, weeks, or months), laboratory technicians characterize longitudinal strains (index strains obtained over the time of infection) (12). This methodology is based on the **I**ndependent **A**ction **H**ypothesis (IAH), which

states that a group of microorganisms inoculated in a host passes through anatomic barriers and the immune system (bottleneck), and the survivors act independently with a defined and finite probability of causing infection (13). Therefore, a homogenous infectious population is assumed (genotypically and phenotypically identical and therefore clonal populations).

The study of longitudinal strains of *C. glabrata* from patients with candidemia has provided valuable information about microevolution within the host and an understanding of how variability occurs over time. During candidemia, the strains can adapt to different selective pressures inside the host (for example, fluconazole therapy), and **g**ain-of-**f**unction (GOF) mutations can occur in genes related to antifungal resistance (14–17). Misas *et al*., (2024) studied 82 serial isolates of *C. glabrata* from 33 patients. They employed the WGS and determined the relationship between isolates from the same patient by phylogenetic analysis based on the amount of SNP's (clonal origin). Twenty-one echinocandin-resistant and 24 fluconazole-resistant strains were discovered, which hold mutations in *FKS1*, *FKS2*, and *PDR1*, respectively. This study demonstrated that CSP^R or/and FCL^R strains have a clonal origin from a susceptible strain, demonstrating that microevolution takes place during therapy with antifungals.

Previously, our research group studied five sequential clinical isolates from one patient, which were collected from two different anatomical sites (four strains from blood and one strain from urine) and even though that all isolates share a clonal origin we found variability at genotypic and phenotypic levels among them, mainly in terms of resistance to antifungals. The strains from blood are FLC^R and CSP^S, but the strain from urine is CSP^R and FLC^S (17).

On the other hand, Cheng *et al*., (2022) and Badrane *et al*., (2023) described the relevance of studying contemporaneous strains (multiple index strains obtained from a single clinical sample at a specific time point during the infection), which, unlike longitudinal strains, are collected at the same point in time. Badrane *et al.* studied 94 contemporaneous strains of *C. glabrata* obtained from 10 patients. They determined their clonal origin and the number of SNPs by WGS. Moreover, they characterized the strains of two patients (patients J and L), which showed major

genotypic and phenotypic variability. Patient J presented two colony morphologies: normal colony variants (NCV) and small colony variants (SCV). These SCVs displayed mitochondrial dysfunction and resistance to fluconazole. Strains from patient L are NCV, and some of them were resistant to azoles due to mutations in *PDR1,* which encodes the Pdr1 transcription factor that regulates transcription of the genes that encode the main efflux-pumps like *CDR1*, which pump fluconazole out of the cell. They demonstrated with this study that phenotypic and genotypic variation may be present in contemporaneous strains. This phenomenon also has been reported in contemporaneous strains of carbapenem-resistant *Klebsiella pneumoniae* (19). This shows that when the characterization is limited to a single index strain, assuming IAH, it may lead to an underestimation of antifungal or antibiotic resistance.

This study aims to identify and characterize 5 contemporaneous strains of *C. glabrata* belonging to 13 patients obtained from two anatomical sites (blood and urine). We identified 77 *C. glabrata* contemporaneous strains where all of the isolates from each individual patient shared a clonal origin, as judged by MLP and *EPA1* markers and the RAPD method. In addition, we found genotypic and phenotypic differences among the contemporaneous strains obtained from three patients (P6, P17, and P18), mainly in antifungal resistance, and these strains were selected for further analysis. We also analyzed four strains from patient 17, which have mitochondrial dysfunction and are unable to grow in the non-fermentable carbon source glycerol (Gly-), known as “petite” cells. We employed a Mitotracker Green fluorescent dye to identify the mitochondrial network in these strains. Finally, we sequenced the *PDR1* gene from three strains from P17 (one strain) and P18 (two strains) to determine if GOF mutations in this gene are responsible for the FLC^R phenotype. Overall, we found phenotypic and genotypic variability in *C. glabrata* contemporaneous strains may exist, and this implies an underestimation at the clinical level in the context of antifungal resistance and treatments for the patient.

Materials and methods

1. *C. glabrata* strains

The reference strains of the Molecular Microbiology Laboratory, DBM, IPICYT, BG14, and CBS138 (ATCC2001) were used as controls for the identification and genotypification of *C. glabrata* contemporaneous strains from clinical samples with 3 sets of species-specific primers for *C. glabrata* (Cg1, Cg2, and Cg3) (20), 3 sets of primers for *ERG3*, *MT-I*, and *RPM2* molecular markers, 3 primers (OPA-18, OPE18, and OPA-09) for the RAPD method, and Oligonucleotides No. *EPA1* (INT) 2059 Fw and *EPA1* (INT) 2060 Rv for amplification of the *EPA1* minisatellites (Table 8), and characterization under different stresses.

Strains used as controls in the semi-quantitative analysis are shown in Table 9.

2. Selection of contemporaneous strains from clinical samples

All the contemporaneous strains were recovered from clinical samples from the collection of Molecular Microbiology of Fungi Laboratory, DBM, IPICYT, Instituto Nacional de Ciencias Médicas, Nutrición Salvador Zubirán, and Hospital Central Dr. Ignacio Morenos Prieto.

Clinical samples were inoculated on YPD broth (Yeast extract 10 g/L, Peptone 10 g/L, and Dextrose 2%) for 24 hours at 30°C. Subsequently, OD_{600} was adjusted to 1.0. Next, serial dilutions from 10^{-4} to 10^{-5} were made, and 100 µL were inoculated in YPD plates. Each plate was grown for 5 days, and 5 colonies were recovered from both plates and stored in glycerol 15% at -71°C.

A total of 77 *C. glabrata* contemporaneous strains were recovered, of which 35 are from blood cultures and belong to three patients (P6, P8, and P13) and 42 are from urine cultures and belong to eight patients (P16, P17, P18, P19, P21, P22, and P23) (Table 1).

3. DNA extraction

We used the FastPrep®-24 (MP Biomedicals) DNA extraction method to obtain genomic yeast DNA, which is standardized in our laboratory. We inoculated each strain in 5 mL of YPD broth and incubated it at 30°C for 24 hours. Next, we recovered

the cell suspension by centrifugation, and 500 µL of buffer A (Tris HCl 50 mM, EDTA 10 mM, NaCl 150 mM, Triton 1%, and SDS 1%) and 500 µL of phenol: chloroform:isoamyl alcohol were added. Then, the samples were placed in FastPrep for 1 second at 4 m/s. We centrifuged and recovered the aqueous phase and added 15 µL of NaCl 5 M and 1 mL of 100% ethanol. The pellets were washed once with 70% ethanol, and 0.2 µL of RNAase cocktail mix (RNase A: 0.1 U/mL and RNase T1: 4 U/mL, Ambion®) were added to the samples and incubated at 37°C for 30 minutes. Finally, the samples were resuspended in 200 µL of Tris 10 mM.

4. Identification of *C. glabrata* contemporaneous strains by species-specific primers

To test the identity of contemporaneous strains of *C. glabrata* recovered from clinical samples, we performed an end-point PCR using 3 sets of *C. glabrata* species-specific primers (Cg1, Cg2, and Cg3), following a modified methodology described by Hernández-Carreón *et al*., 2021. Each reaction was performed using a purified homemade DNA polymerase in the Molecular Microbiology Laboratory, and the reaction mix was adjusted to a total volume of 20 µL. For the electrophoresis,10 µL from each reaction was loaded into a 1.5% agarose gel and run at 100 V for 40 minutes.

Likewise, we determined the presence of other *Candida* spp. in the clinical sample and contemporaneous strains by end-point PCR using specific primers to *C. albicans* (Ca6), *C. tropicalis* (Ct), and *C. parapsilosis* (Cp). Each reaction was performed using a purified homemade DNA polymerase, and the reaction mix was adjusted to a total volume of 20 µL. For the electrophoresis,10 µL from each reaction was loaded into a 1.5% agarose gel and run at 100 V for 40 minutes.

5. Genotyping of *C. glabrata* contemporaneous strains by MLP, RAPD, and *EPA1* microsatellites

To determine whether the contemporaneous strains have a clonal origin, we employed an end-point PCR using 3 sets of primers addressed to three molecular markers, which are RPM2, MT-I, and ERG3, previously described by Foulet *et al.*, (2005), to amplify polymorphic microsatellites. The reaction conditions were

obtained from López Marmolejo et al. (2021) master's thesis. Each reaction was performed using homemade polymerase DNA and adjusted to a total volume of 20 µL. For the electrophoresis, 10 µL from each reaction was loaded into a 1.8% agarose gel. To determine the sizes of each PCR product, software ImageJ® was used, and a dendrogram was made using the R programming language with the *hclust* function.

Likewise, we used the RAPD method with 3 single primers, which are OPA-18, OPE-18, and OPA-09, to genotype the strains from patient 6, patient 17, and patient 18 to confirm their clonal origin. The reaction conditions were obtained from López Marmolejo *et al*., (2021). The total volume for each reaction was 20 µL, and then 10 µL was loaded into a 1.5% agarose gel and run at 100 V for 45 minutes. We used a binary matrix (1 or 0) to identify the patterns of presence or absence of PCR products, and a dendrogram was constructed with the R programming language.

Finally, we amplified the microsatellites of *EPA1* in the ORF. The reaction conditions were obtained from Herrera Basurto *et al*., (2020), and the provider instructions of Dream Taq Green Polymerase (Thermo Fisher Scientific). The total volume for each reaction was 5 µL, and the total volume of the samples was loaded into a 2.0% agarose gel.

6. Phenotypic characterization of *C. glabrata* contemporaneous strains

To characterize the ability of contemporaneous strains to respond to different stresses, we performed a spot-growth assay under different conditions.

First, we tested all 77 *C. glabrata* contemporaneous strains. The strains were grown in 5 mL of YPD broth for 48 hours at 30 °C to ensure the strains were in the stationary phase. OD_{600} was adjusted to 0.1 and 0.05. We spotted each cell suspension using a replicator of 12x8 pins on plates with FLC (4, 8, 16, 32, and 64 µg/mL), CSP (0.0125, 0.025, and 0.05 µg/mL), different temperature (30, 37, 44, and 45°C), H_2O_2 (5, 10, and 15 mM), caffeine (5, 10, 15, and 20 mM) and YPG (2%).

Finally, we selected three patients (P6, P17, and P18) whose contemporaneous strains showed phenotypic differences, and a spot-growth assay was performed with ten-fold serial dilutions from OD_{600} 1.0 to 10^{-5} in a 96-well plate to determine resistance or susceptibility to different conditions. Each cell suspension was spotted

on plates with FLC (8, 16, 32, 64, and 128 µg/mL), CSP (0.0125, 0.025, 0.035, and 0.05 and 0.07 µg/mL), temperature (30, 37, 44, and 45°C), H_2O_2 (5, 10, and 15 mM), caffeine (5, 10, 15, and 20 mM) and YPG (2%).

7. Sequencing of the *PDR1* gene of *C. glabrata*

To identify if GOF mutations in the *PDR1* gene are responsible for the FLC^R phenotype in the strains from P17 and P18, we selected and sequenced the *PDR1* gene in two strains from each patient (P17: SL339 and SL385; P18: SL354 and SL357).

Genomic DNA from each strain was used as a template to amplify the *PDR1* gene with a primer set PDR1@-635 bp FW and PDR1@789 bp RV (Table 3) by end-point PCR using iProof polymerase (BIORAD). The reaction mix was adjusted to a total volume of 50 µL. The PCR products were purified by DNA precipitation. 50 µL of each reaction were loaded on a 0.8% agarose gel. Next, we cut and crush the bands, and 500 µL of phenol:chloroform:isoamyl alcohol and 300 µL of sterile water were added. We homogenized and centrifuged the mix at 12,000 rpm for 10 minutes at 4°C. Subsequently, 30 µL of sodium acetate (3 M, pH: 5.5) and 400 µL of isopropanol were added and incubated at -20°C overnight. We washed with 800 µL ethanol once and centrifuged (12,000 rpm for 10 minutes at 4°C). Finally, we resuspended the PCR products in 30 µL of sterile water. The sequencing was performed by the Genetic Analyzer 3500 and 3130 at LANBAMA, IPICYT (Applied Biosystems).

8. Mitochondrial staining with MitoTracker™ Green dye

To observe the mitochondrial morphology in the petite P17-derived strains, we employed MitoTracker™ Green FM (Thermo Fischer Scientific).

The petite strains, one Gly+ (SL339) from the same patient, and BG14, were grown overnight in YPD, YPD + FLC and YPG. Then, the cell suspension was adjusted to an OD_{600} of 1.5 in CAA and incubated for 2 hours at 30°C. The cells were washed once in sterile water after which we added 100 µL of 1x MitoTracker™ Green FM and incubated for 30 minutes. Finally, the cells were observed using a fluorescence microscope Zeiss Axio Vision Blue 204 edition.

Results

1. Identification of 77 contemporaneous clinical strains of *Candida glabrata* using species-specific primers

Several *Candida* spp. are responsible for systemic candidiasis, and *C. glabrata* is the second most common species, just after *C. albicans,* in the USA, Latin America, and northern Europe (24–26). We decided to characterize contemporaneous clinical strains of *C. glabrata* obtained from individual clinical blood and urine samples provided by the Instituto Nacional de Ciencias Médicas and Nutrición Salvador Zubirán in Mexico City and Hospital Central Dr. Ignacio Morones Prieto in San Luis Potosí.

We first recovered 87 contemporaneous strains from several clinical samples and plated them on rich medium (YPD plates). No clear phenotypic differences were observed among the colonies obtained. Next, we performed PCR with three sets of species-specific primers to *C. glabrata* (Cg1, Cg2, and Cg3) for their mycological identification (20).

Ten strains from two patients (P14 and P15) did not amplify with Cg primers. These strains were identified as *C. albicans* based on the amplification with the *C. albicans* species-specific primers and the ITS (Internal Transcribed Sequence) and were discarded (Supplementary Figure S1). The rest of the 77 contemporaneous strains from 11 patients (35 from blood and 42 from urine) were identified as *C. glabrata* as they were positive for each primer set. Supplementary Figure S2 shows an example of *C. glabrata* identification from patient 17. Table 1 shows the identification of all the contemporaneous strains.

2. *C. glabrata* contemporaneous strains from each patient share a clonal origin

Prolonged hospitalization and inappropriate antifungal therapy of patients can cause mixed fungemia (27,28). In fact, patients can acquire systemic candidiasis, not only from their own microbiota, but also from surgeries or contaminated medical devices; so infections with more than one strain of *C. glabrata* may occur (29–32). To study phenotypic and genotypic variation within isolates obtained from individual clinical samples (contemporaneous isolates), it is crucial to determine whether several

colonies obtained from each clinical sample share a clonal origin to discard a mixed candidemia.

We first genotyped the 77 contemporaneous strains of *C. glabrata* with three molecular markers based on microsatellite length polymorphism (MLP): *RPM2*, *MT-I*, and *ERG3* molecular markers, which contain conserved tandem repeats that exhibit copy number polymorphisms between different strains (21).

We found no differences among the alleles of *C. glabrata* contemporaneous strains for each molecular marker. Figure 1A shows an example of PCR products from P6. We determined the relative distances migrated from the top to the edge of the PCR products in the agarose gel, using a standard curve determined the sizes of the PCR products using Image J®. . Next, we constructed dendrograms with the *hclust* function in the R programming language with the product sizes determined by Image J®. Each contemporaneous strain is clustered within a phylogenetic clade and clustered separately from the reference strains, suggesting a clonal origin. Supplementary Figure 3 shows an example of the phylogenetic trees from P6 (blood) and P18 (urine). The results of these analyses for all the patients are presented in Table 1. This data suggests that the contemporaneous strains from each patient share a clonal origin.

We then compared the relationship among groups of contemporaneous strains from blood and urine clinical samples from the same patient and the same date to determine if such a phylogenetic relationship is conserved. To achieve this, we constructed dendrograms with the product sizes previously obtained from Image J® for each molecular marker of each patient and clinical sample. The contemporaneous strains of blood and urine were grouped in a clade by the patient they were obtained. Therefore, the relationship among the strains is conserved even though the strains were compared with more clinical strains that were cultured in different hemoculture bottles (Figure 1B and 1C).

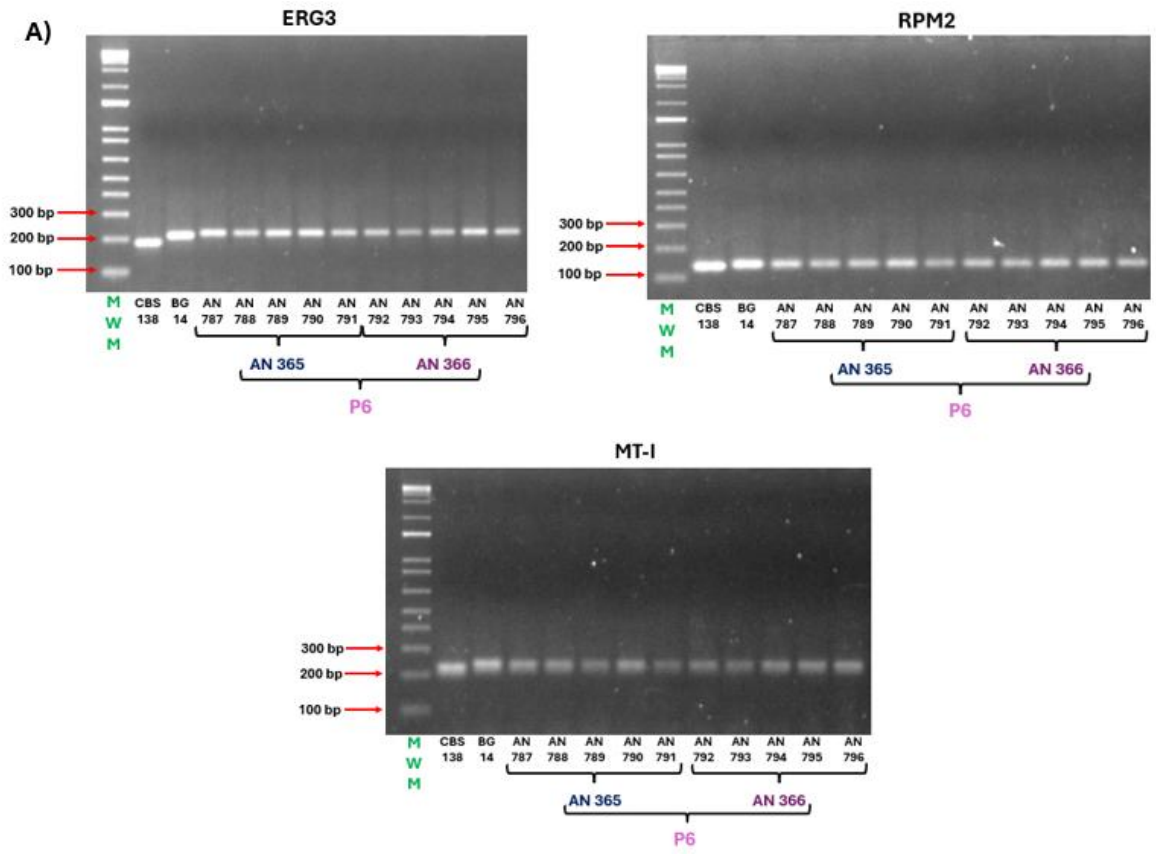
A)
ERG3
RPM2
MT-I
300 bp
200 bp
100 bp
M
W
M
CBS 138
BG 14
AN 787
AN 788
AN 789
AN 790
AN 791
AN 792
AN 793
AN 794
AN 795
AN 796
AN 365
AN 366
P6

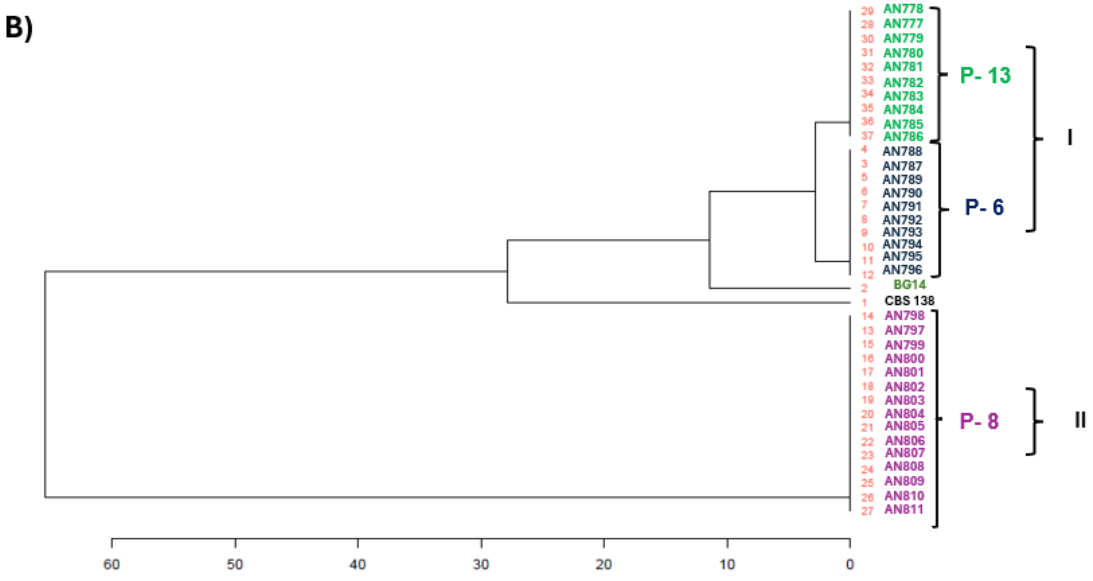
B)
AN778
AN777
AN779
AN780
AN781
AN782
AN783
AN784
AN785
AN786
AN788
AN787
AN789
AN790
AN791
AN792
AN793
AN794
AN795
AN796
BG14
CBS 138
AN798
AN797
AN799
AN800
AN801
AN802
AN803
AN804
AN805
AN806
AN807
AN808
AN809
AN810
AN811
P- 13
P- 6
P- 8
I
II
60
50
40
30
20
10
0

266

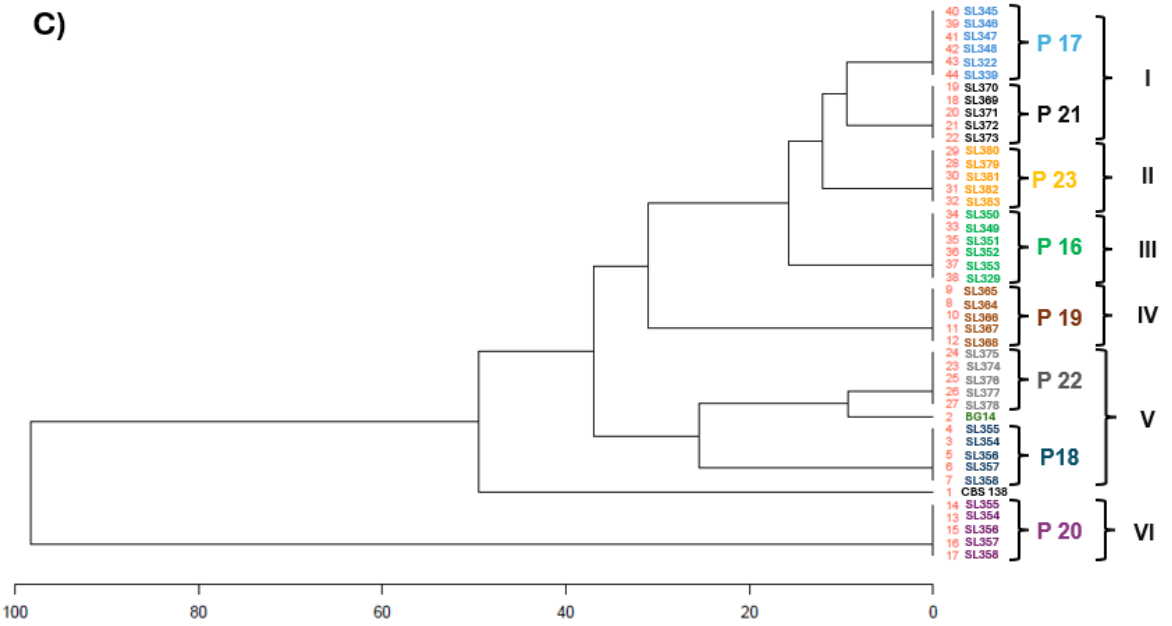

Fig. 1. Genotyping with *ERG3*, *RPM2*, and *MT-I* molecular markers from P6 and phylogenetic relationship among *C. glabrata* contemporaneous strains from blood and urine clinical samples.

A) *ERG3*, *MT-I*, and *RPM2* molecular markers are based on microsatellite length polymorphisms (MLP). P6 consists of two blood clinical samples from the same date (AN365 and AN366), and five contemporaneous strains were obtained for each sample. No differences in the sizes of PCR products were found among these contemporaneous strains for each marker, however, the PCR product sizes were different compared to CBS138 and BG14 strains. **B)** MLP markers analyzed with Image J® and RStudio® were used to construct a dendrogram to determine the relationship among the contemporaneous strains from P6, P8, and P13. P6 and P13 consist of two clinical samples, and P8 of three clinical samples. The clinical strains obtained from each patient are clustered in a clade according to the patients they were obtained from. The strains from P6 and P13 are grouped in genotype I, whereas P8-derived strains are clustered in genotype II. **C)** Image J® and RStudio® were used to construct a dendrogram to determine the relationship among the contemporaneous strains from P16 to P23 these strains are grouped in six genotypes.

We also used the RAPD method to confirm the genetic relatedness of the contemporaneous strains derived from P6, P17 and P18. This method has been used to genotype different *Candida* spp. using several short primers (33–35). We employed primers OPA-18, OPE-18, and OPA-09 as well as the tandem repeat region located in the ORF of the *EPA1* gene to confirm the clonal origin of contemporaneous strains from individual patients. This region is formed by 3 repeats of 40 amino acids each which are rich in Serine-Threonine (S-T), corresponding to 360 nucleotides. However, these repeats can vary in length among clinical strains (36,37). We decided to confirm the clonal origin from isolates derived from P6, P17, and P18 contemporaneous strains, using the RAPD method with OPA-18, OPE-18, and OPA-09 primers and the microsatellites in the ORF of the *EPA1* gene.

None of the contemporaneous strains show differences in the amplification patterns with the three RAPD primers, but the patterns were different from those from CBS138 and BG14 (Supplementary Figure S8). We made a binary matrix according to the presence or absence of the PCR products and constructed a phylogenetic tree using ImageJ and the *hclust* function. For *EPA1* amplification, a similar phenomenon was observed. The PCR products from each patient showed the same size between them but differed from the reference strains. We decided to compare a representative contemporary strain from each patient (P6, SL17 and SL18) with other patients previously analyzed from our laboratory collection (P2 and P4). The PCR products of contemporaneous strains from this work were different from the strains derived from P2 and P4. The strains from P4 had similar amplification size to CBS138 and BG14 (Supplementary Figure S7).

3. Contemporaneous strains from P6, P17, and P18 displayed phenotypic variability

C. glabrata has different virulence factors necessary to adapt and cause infection in a susceptible host. These virulence factors include a strong response to oxidative stress, resistance to heat shock, to antifungals, high capacity to adhere to host cells and medical devices. These attributes are mediated by stress response pathways, epigenetic mechanisms, and mutations, which can confer higher resistance to

different environments that challenge the pathogen (11,38–40). However, these mechanisms may differ among strains even if they have a clonal origin (18).

We screened the response of the 77 contemporaneous strains from 11 patients to oxidative stress, heat shock, and two antifungals to determine if there is phenotypic variability among them. We started from stationary phase cultures of each contemporaneous strain and adjusted each cell suspension to either OD_{600} 0.1 or 0.05. We then spotted each cell suspension on YPD plates under different conditions.

3.1 Blood Samples: Contemporaneous strains from P6 display phenotypic variability regarding antifungal susceptibility, hydrogen peroxide, and temperature resistance

Samples obtained from P6, P8, and P13 are derived from blood cultures. All strains belonging to P8 were susceptible to fluconazole (FLC^S) at 16 µg/mL, but they did not show differences with each other in the rest of the evaluated conditions. All of the strains from P13 were able to grow on FLC at 32 µg/mL (FLC^{SDD}), similar to BG14. Also, these contemporaneous strains from P13 were able to grow on caspofungin at 0.05 µg/mL (CSP^R), and thermotolerant at 45°C. However, in P6, one strain was FLC^S at 16 µg/mL compared to the contemporaneous strains from the same clinical sample (AN366), but this strain also showed CSP^S at 0.025 µg/mL, sensitivity at 37°C, sensitivity to H_2O_2 at 15 mM, and sensitivity to caffeine at 15 mM. All of the strains from this patient were able to grow on YPG (with glycerol as carbon source) (Supplementary Figures S2A-S2D).

3.2 Urine Samples: Contemporaneous strains from P17 and P18 display phenotypic variability

Clinical samples from P16 to P23 are derived from urine. In P18, one contemporaneous strain (SL357) was FLC^R to 64 µg/mL, resistant to 20 mM caffeine, and resistant to 0.05 µg/mL of CSP, as well as to a temperature of 45°C (Supplementary Figures S5A-D). Additionally, four strains from P17 (SL345, SL346, SL347, and SL348) were FLC^R to 64 µg/mL and resistant to 20 mM of caffeine (Supplementary Figures S5A and S5C). Initially, these four strains did not grow on

YPG, suggesting that these strains have mitochondrial dysfunction called “petites”. However, when we grew the strains in YPG for the second time, the SL346 clinical isolate showed growth in YPG (Supplementary Figure S6). To identify the rate at which this switch occurs in the clinical isolate, we performed an experiment using 10 independent cultures of the SL346 clinical isolate in YPD rich medium. We then adjusted the OD_{600} to 1.0, and 200 µl of a 10^{-5} dilution were plated in YPD plates. After 48 hours of incubation at 30°C, we performed a replica plate from each plate on YPD and YPG plates (Supplementary Figure S6). In the YPD plates, we observed growth of both small and normal colonies in at least 5 of 10 plates (Table 3). Normal colonies (NCV) could grow on YPG, but the small colonies (SCV) could not grow (Supplementary Figure S6), suggesting that the NCVs have functional mitochondria (Gly+ phenotype), whereas SCVs do not have functional mitochondria (Gly- phenotype). We selected one Gly+ and one Gly- strain (SL384 and SL385, respectively) derived from SL346 for further analysis.

The contemporaneous strains obtained from the other patients exhibited various phenotypes but did not differ between contemporaneous isolates. We focused only on the strains that showed differences among contemporaneous strains.

3.3 Contemporaneous strains from P6, P17, and P18 display phenotypic variability by semiquantitative plate growth assays.

We selected P6, P17, and P18, which showed phenotypic differences between contemporaneous strains, for further analysis using a semi-quantitative growth-spot assay, with 10-fold serial dilutions of cell suspensions starting with an OD_{600} of 0.5 and diluting from 10^{0} to 10^{-5}. The dilutions were spotted on YPD plates under different conditions. We used several mutants in the BG14 background as controls for each condition: *pdr1*Δ (FLC-sensitive), *hst1*Δ (FLC-resistant), *hdf1*Δ (temperature-sensitive), *cta1*Δ (H_2O_2-sensitive), *snq2*Δ (caffeine-sensitive), and CBS138 (temperature-sensitive), AN376 (CSP-resistant), and BG14 (temperature-resistant) as control strains for each condition (Table 9).

Consistent with the previous qualitative analysis, SL345, SL385, SL347, and SL348 from P17, as well as SL357 from P18, were FLC^{R} to 128 µg/mL, whereas the other clonal strains from each patient were susceptible to 16 or 32 µg/mL of FLC

(Figure 2B and 2C). AN794, one of the contemporaneous isolates from P6 showed higher susceptibility to FLC (16 µg/mL) than its four contemporaneous strains (Figure 2A).

Regarding heat stress, only SL357, one of the contemporaneous strains from P18, was resistant to heat stress as it could grow at 45°C, similar to BG14 (Figure 3C). On the other hand, the AN794 from P6 strain grew poorly at 37°C compared to the rest of its contemporaneous strains from this patient (AN792, AN793, AN795, and AN796, Figure 3A). All of the strains from P17 grew similarly under heat stress and were unable to grow at 45°C (Figure 3B).

In the case of oxidative stress, contemporary strains from P17 and P18 did not show differences in susceptibility when exposed chronically to H_2O_2, and all the strains were susceptible to 15 mM, whereas AN794 from P6 was susceptible to 10 mM and 15 mM of H_2O_2 compared with its contemporaneous strains (Figure 4). Moreover, we challenged the strains with caffeine, which is classified as a cell-wall perturbing agent; however, pleiotropic effects have been reported in eukaryotic cells (41). All strains from P6 showed sensitivity to chronic exposure to caffeine at 15 mM, although AN794 grew slowly compared to its contemporaneous strains (Figure 5A). The strains from P17 and P18 that showed resistance to FLC were also resistant to 20 mM caffeine (Figures 5B and 5C). In addition, the strains from P6 and P18 were all able to grow in YPG. On the other hand, we previously identified four “petite” strains in P17, however, some cells from SL345 and SL348 in the semi-quantitative analysis could grow in YPG (Figure 6). We tested many independent colonies from SL345, SL347, and SL348 on YPG, and only SL345 and SL347 showed growth of Gly+ and Gly- strains, while in the plates of SL348, we did not observe any Gly+ growth. At least 5 of the 10 plates of SL345 and SL346 showed NCVs, while in SL347, just 2 plates showed that (Supplementary Figure S5 and Tables 3, 5, and 6). The appearance of Gly+ strains in almost all the initially isolated Gly- contemporaneous strains from P17 suggests that these Gly- cultures are in fact, contaminated with Gly+ strains from the original sample.

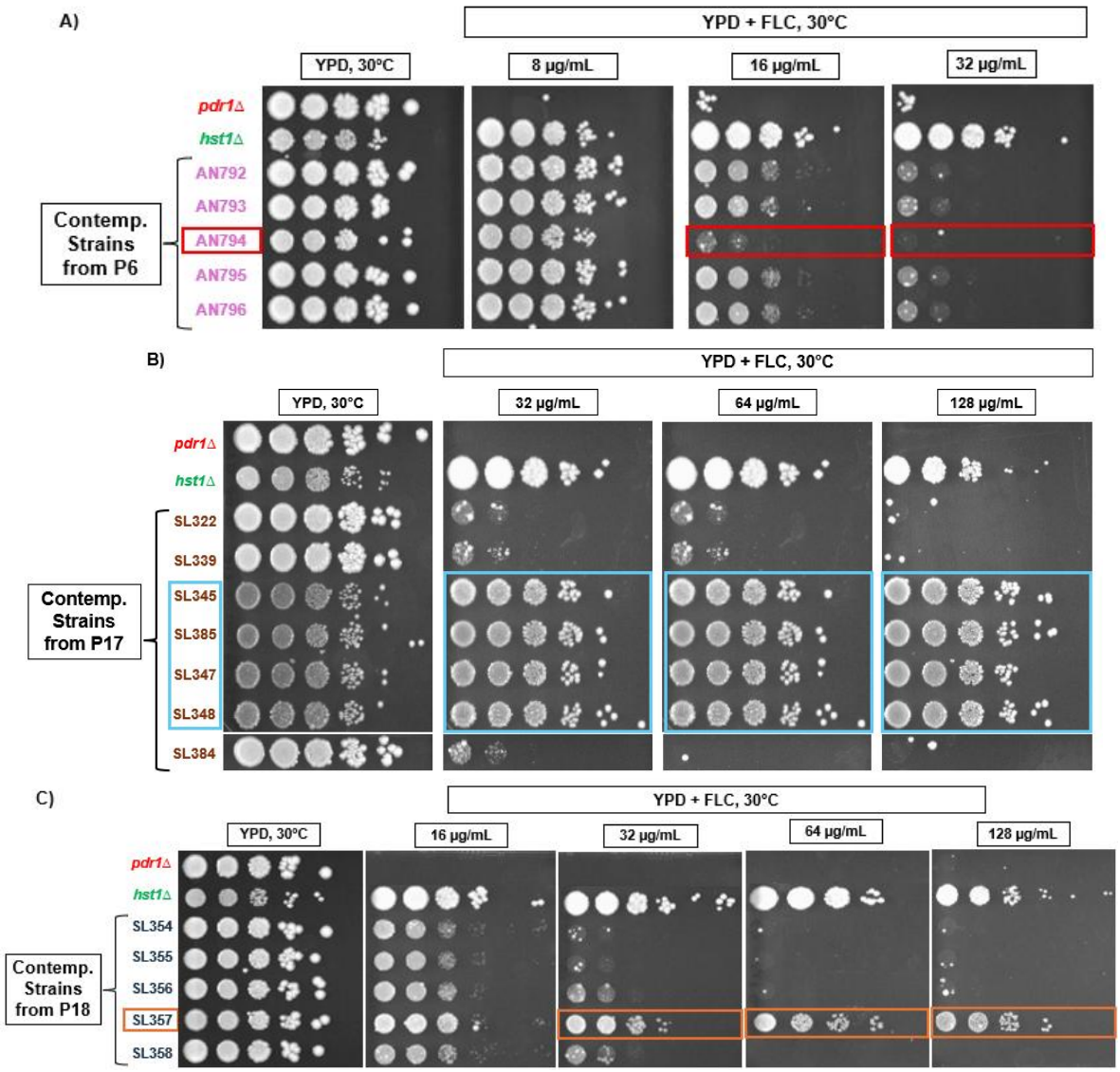

Fig. 2. FLC susceptibility of contemporaneous strains from P6, P17, and P18 by growth-spot assay with serial dilutions.

Stationary phase cultures of *C. glabrata* contemporaneous strains were adjusted at OD_{600}0.5, and 10-fold serial dilutions were made (up to 10^{-5}). We then spotted the cell suspension on YPD plates at different concentrations of FLC (8, 16, 32, 64, and 128 µg/mL). **A)** In P6, one contemporaneous strain (AN794) is FLC^S at 16 µg/mL (red square). **B)** In P17, four strains (SL345, 346, 347, and 348) that are SCV are FLC^R (blue square). **C)** In P18, one strain (SL357) shows FLC^R up to 128 µg/mL; nevertheless, this strain is not SCV (orange square). *pdr1*Δ and *hst1*Δ in the BG14 background were used as controls of susceptibility and resistance to FLC, respectively.

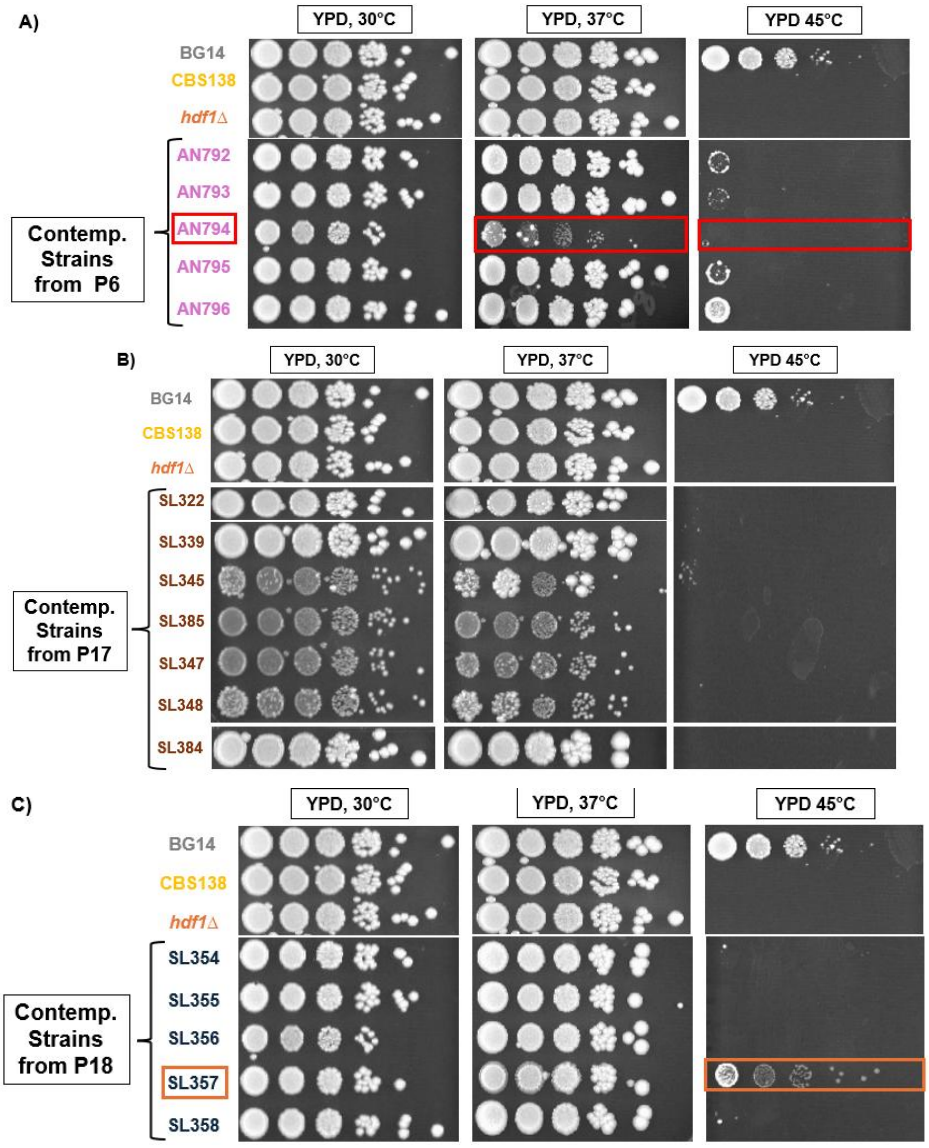

Fig. 3. Heat shock susceptibility of contemporaneous strains from P6, P17, and P18 by growth-spot assay with serial dilutions.

C. glabrata contemporaneous strains were adjusted at OD_{600} = 0.5 and serial dilutions were made until 10^{-5}. We then spotted the cell suspension on YPD agar at three temperatures (30, 37, and 45°C). **A)** AN794 from P6 is more susceptible to 37°C than the other contemporaneous strains (red square), but all the strains are susceptible to 45°C except AN796. **B)** In P17, all the strains did not show differences in growth at any temperature. **C)** In P18, SL357 can grow at 45°C in contrast to the other strains that do not grow under the same condition (orange square). BG14 (resistant to 45°C), CBS138, and *hdf1*Δ (susceptible to 45°C) were used as controls.

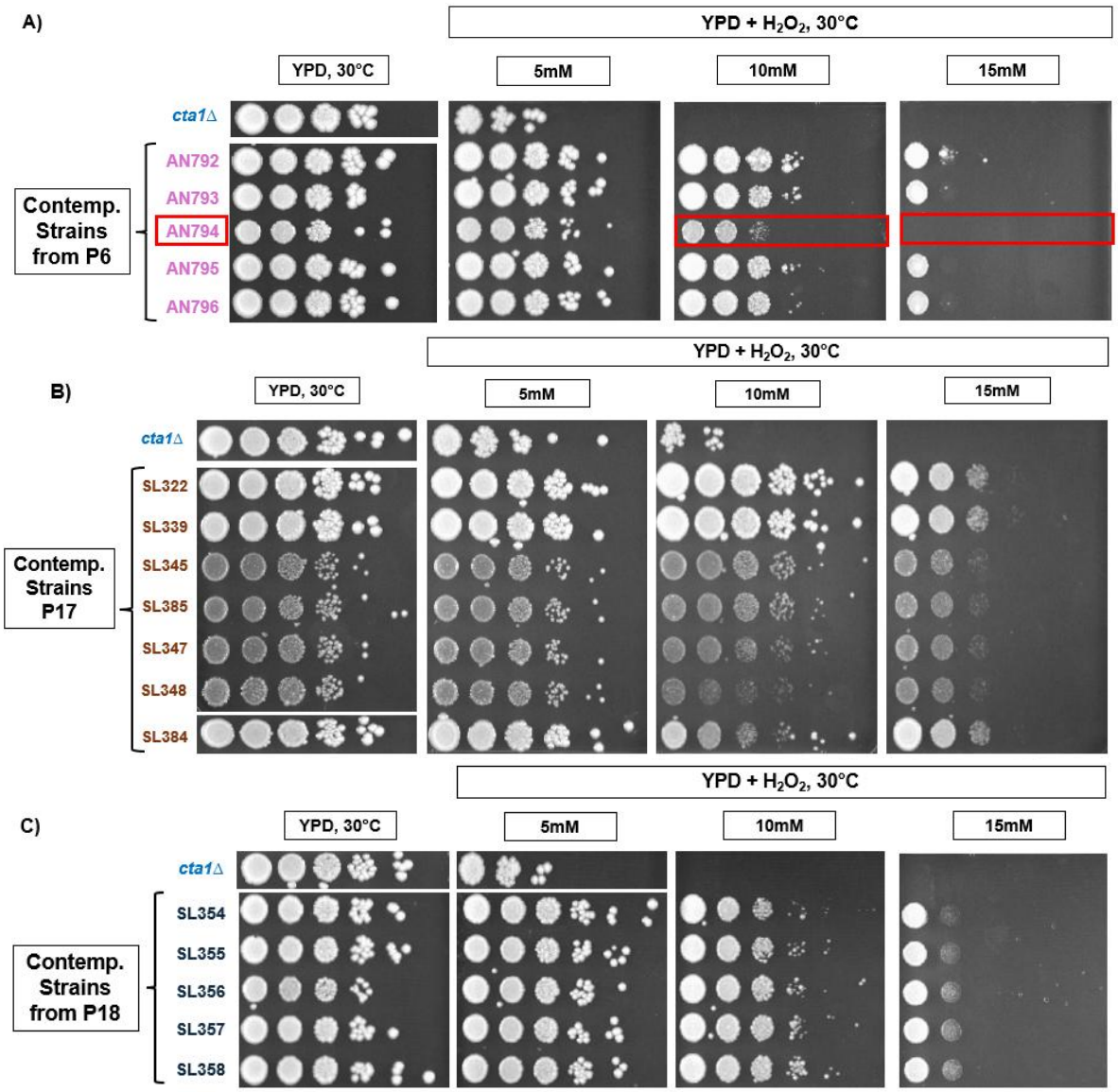

Fig. 4. H_2O_2 susceptibility of contemporaneous strains from P6, P17, and P18. *C. glabrata* contemporaneous strains were adjusted at OD_{600} = 0.5 and 10-fold serial dilutions were made up to 10^{-5}. Then, we spotted the cell suspension on YPD agar at three concentrations of H_2O_2 (5 mM, 10 mM, 15 mM). **A)** AN794 from P6 is more sensitive to 10 mM and susceptible to 15 mM. **B)** There are no differences among contemporaneous strains from P17, in each concentration. **C)** All the strains from P18 are sensitive at H_2O_2 15 mM. *cta1*Δ was used as a susceptibility control.

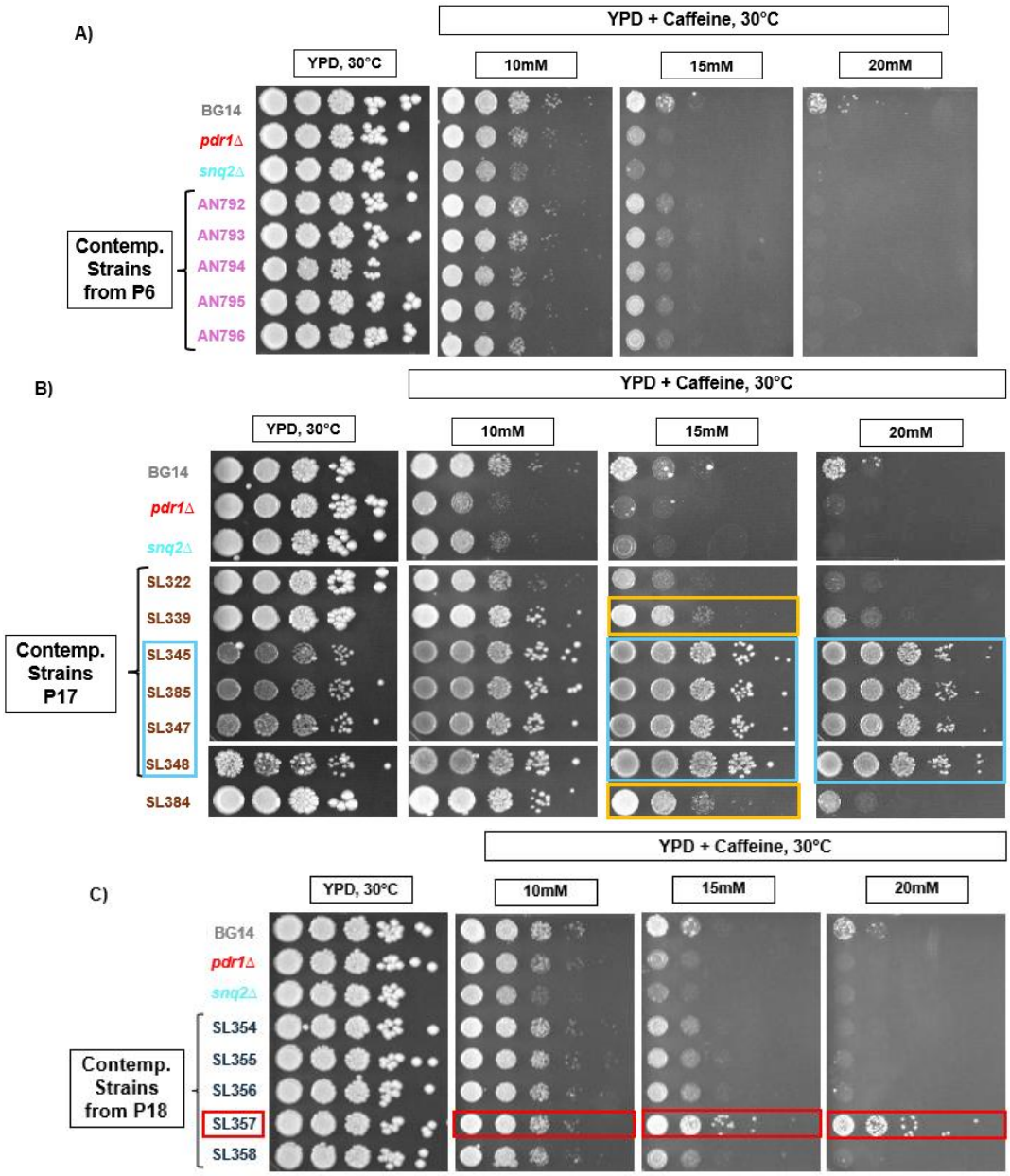

Fig. 5. Caffeine susceptibility of contemporaneous strains from P6, P17, and P18.

C. glabrata contemporaneous strains were adjusted at OD_{600} = 0.5 and 10-fold serial dilutions were made up to 10^{-5}. Then, we spotted the cell suspension on YPD agar at four caffeine concentrations (5, 10, 15, and 20 mM). **A)** Strains derived from P6 showed sensitivity to 15 mM caffeine. **B)** The four petite strains from P17 were more resistant to 20 mM caffeine than their contemporaneous strains. **C)** SL357 derived from P18, was resistant to 20 mM caffeine, whereas the other strains were sensitive at 15 mM.

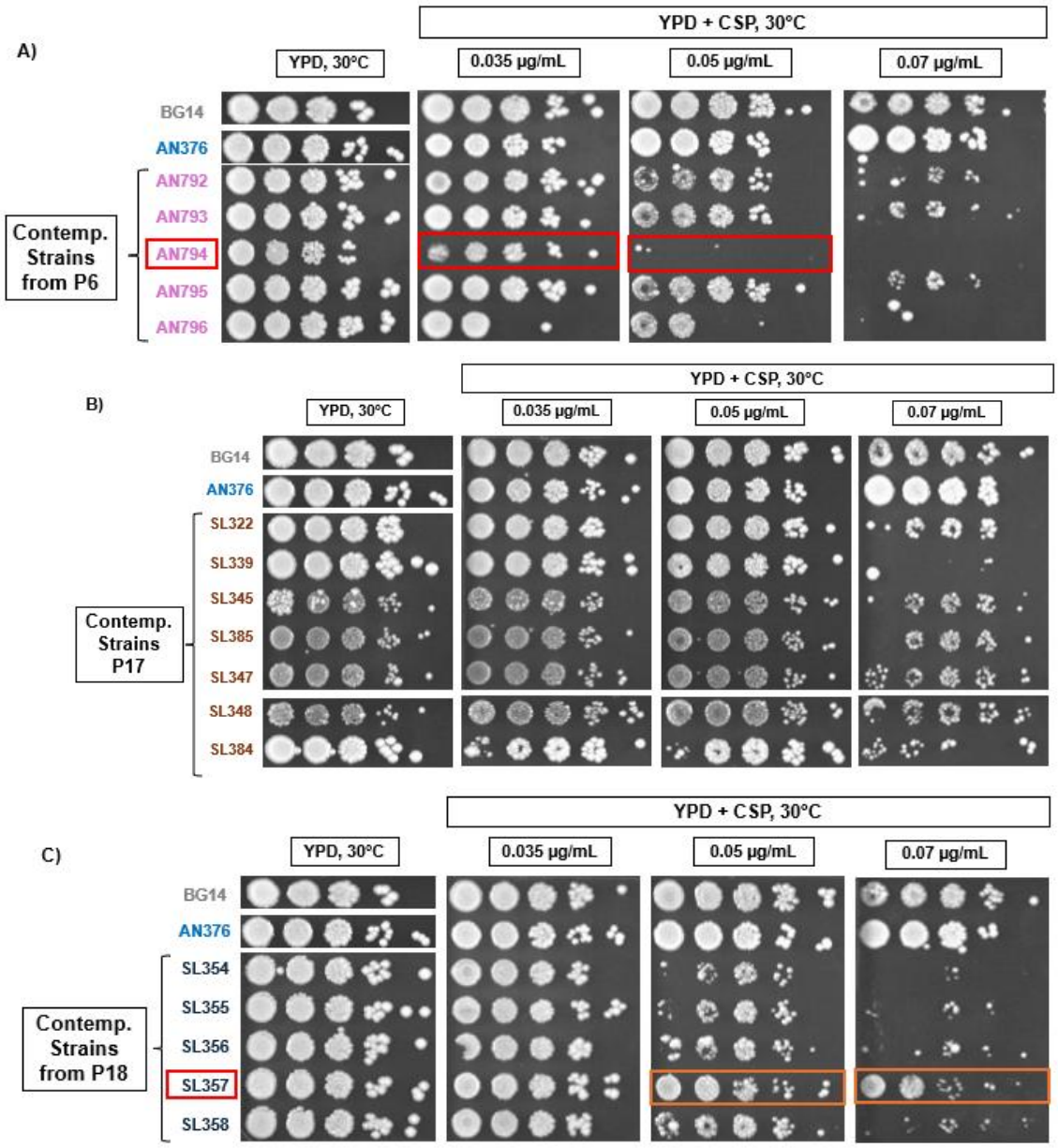

Fig. 6. Caspofungin susceptibility of contemporaneous strains from P6, P17, and P18.

C. glabrata contemporaneous strains were adjusted at OD_{600} = 0.5, and 10-fold serial dilutions were made up to 10^{-5}. Then, we spotted the cell suspension on YPD agar at four caspofungin concentrations (0.025, 0.035, 0.05, and 0.07 µg/mL). **A)** The strain from P6 AN794 was more susceptible to 0.035 µg/mL of CSP compared to its contemporaneous strains. **B)** SL339 from In P17 was CSP-susceptible compared to its contemporaneous strains at 0.07 µg/mL. **C)** SL357, derived from P18, was more resistant to 0.07 µg/mL of CPS, whereas its contemporaneous

strains did not grow at this concentration. BG14 (CSP^S) and AN376 (CSP^R) were used as resistance controls.

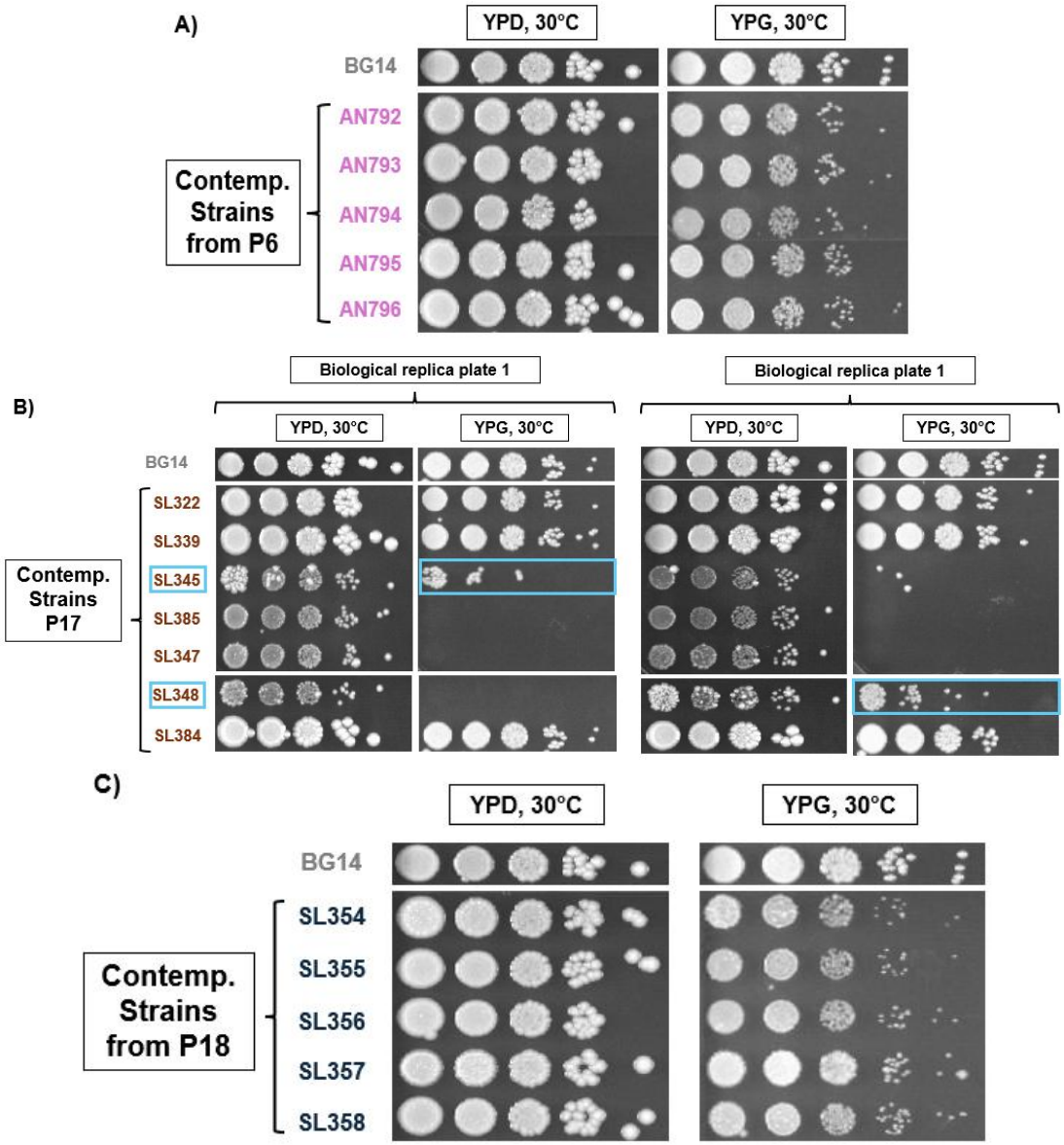

Fig. 7. Ability to use glycerol as a non-fermentable carbon source of contemporaneous strains from P6, P17, and P18.

C. glabrata contemporaneous strains were adjusted at OD_{600} = 0.5, and 10-fold serial dilutions were made until 10^{-5}. Then, we spotted the cell suspension on YPD agar with glycerol as a carbon source (2%). **A)** The contemporaneous strains from P6 did not show differences in YPG-growth. **B)** Four strains from P17 were classified as petites (SL345 to SL348). Although SL345 and SL348 displayed a petite phenotype, some cells can grow in YPG and form colonies. SL345 showed the same

phenomenon in the same condition (blue squares). **C)** Clinical strains from P18 did not show differences in YPG-growth.

4. The four P17-derived "petite" strains showed diffuse mitochondrial staining with MitoTracker™ Green FM

C. glabrata "petite" strains are characterized by partial or complete loss of mitochondrial DNA (mtDNA), leading to respiratory deficiencies and, therefore, are incapable of growing in non-fermentable carbon sources and slow growth in glucose. However, they have clinical relevance due to their considerably lower susceptibility to azoles due to overexpression of the *PDR1* gene, which encodes the transcriptional activator of some genes encoding efflux pumps like Cdr1 and Cdr2. this implies a challenge to treat the infection (18,42–46).

P17 contains four "petite" strains (SL345 to SL348) because they cannot grow in YPG. To determine the morphology of mitochondria, we employed MitoTracker™ Green FM. This dye can cross passively the mitochondrial membrane and accumulate in active mitochondria. Specifically, the dye binds to mitochondrial proteins (e.g., cytochrome C) through the thiol groups in the inner membrane (47). In reference BG14 and SL339 (a contemporaneous Gly+ strain from P17), fluorescence intensity was significantly higher than in the four petite strains from the same sample. In both strains, a mitochondrial network and localized fluorescent points can be appreciated (Figure 7). On the other hand, the fluorescence intensity in the SL345 to SL348 petite strains is significantly reduced, and the characteristic points were not observed. Moreover, the low fluorescence is not localized, instead, a diffuse signal throughout the cells is observed (Figure 7). Despite some colonies from the SL345 and SL348 strains growing in YPG, we could not observe the mitochondrial network among them.

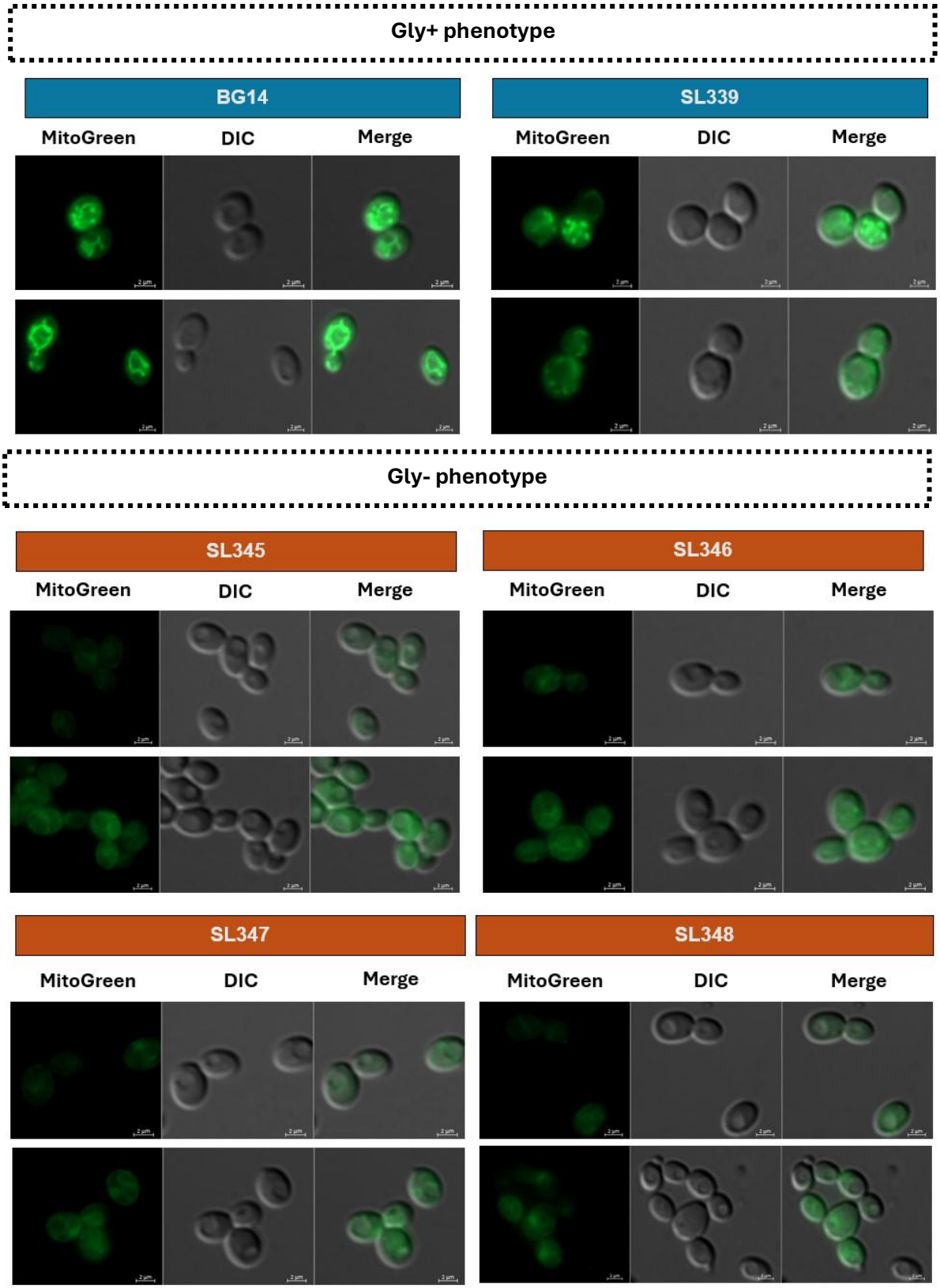
Gly+ phenotype
BG14
MitoGreen
DIC
Merge
SL339
MitoGreen
DIC
Merge
Gly- phenotype
SL345
MitoGreen
DIC
Merge
SL346
MitoGreen
DIC
Merge
SL347
MitoGreen
DIC
Merge
SL348
MitoGreen
DIC
Merge

488

Fig. 8. MitoTracker™ Green FM micrographs of Gly+ and Gly- contemporaneous strains from P17.

The four *C. glabrata* "petite" strains (SL345 to SL348), which are Gly-, and one Gly+ strain (SL339) derived from P17, were stained with MitoTracker™ Green FM and observed under a fluorescence microscope Zeiss Axio Vision Blue 204 edition. In BG14 and SL339, mitochondria are clearly stained as a mitochondrial network or localized points. Meanwhile, the four Gly- strains showed low intensity and diffused fluorescent staining.

5. *PDR1* gene from SL357 (Gly+ from P18) and SL385 (Gly- from P17) harbored two polymorphisms not responsible for FLC-resistance phenotype

Resistance to antifungals in *C. glabrata* is considered one of the key virulence factors in clinical settings and is the primary cause of persistent candidiasis. This resistance has been increasing over the years due to the widespread use of antifungals, with fluconazole being the most common antifungal used to treat candidemia (9,48). In *C. glabrata*, gain-of-function mutations (GOF) in the *PDR1* gene, which encodes the transcription factor Pdr1, are a major cause of acquired resistance to FLC, as these GOF mutants result in strong induction of genes encoding the major efflux pumps such as Cdr1 and Cdr2 (49–51).

SL357 strain derived from P18 is resistant to high concentrations of FLC (Fig. 2), and it's not petite (Gly+ phenotype); so, we decided to sequence the *PDR1* gene from this strain to determine whether GOF mutations in this gene are the cause of the FLC^R phenotype. We also sequenced the SL354 strain from P18, which displayed FLC^S and Gly+ phenotypes, and SL385 from P17, which is Gly- (petite phenotype) and FLC^R.

We compared the nucleotide and amino acid sequences of these strains with the previously sequenced CBS138 and BG14. The *PDR1* sequences from strains derived from our patients were aligned using MacVector software. The sequences from SL385 and SL357 Pdr1 show the same length as CBS138 and BG2, and they have 99.7% similarity with CBS138 and 99.8% similarity with BG2. We compared the amino acid sequence and found that Pdr1 harbored two polymorphisms, S76P and T143P. These mutations are not located in any described domain of Pdr1 (52).

These mutations are very common among clinical isolates from different geographic zones and importantly, have not been reported as GOF mutations conferring resistance to FLC in clinical isolates, as they are present in both sensitive and resistant FLC clinical isolates, and they are almost always present together (14,51–54).

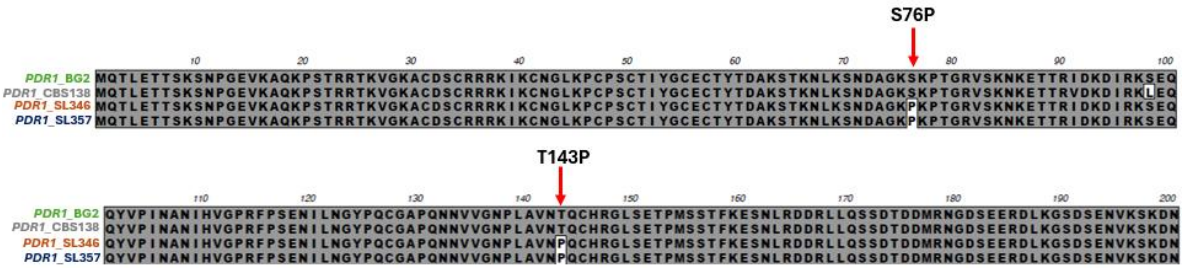

Fig. 9. Amino acid alignments of Pdr1 from SL385 (P17) and SL357 (P18) clinical isolates.

The *PDR1* genes from SL385 (FLC^R Gly- from P17) and SL357 (FLC^R Gly+ from P18) were sequenced using the Genetic Analyzer 3500 and 3130. These sequences were constructed using the *PDR1* gene from CBS138. In addition, they were aligned and compared against BG2 and CBS138 Pdr1 amino acid sequences. SL385 and SL357 harbored S76P and T143P mutations, which are not located in any identified domain of Pdr1.

Discussion

The global burden of fungal diseases has increased quickly due to the rise in the immunocompromised population; such infections have high mortality rates, killing a million people worldwide, where candidiasis represents one of the most common causes of nosocomial and bloodstream infections, with 400,000 – 700,000 cases reported annually (55,56). *C. glabrata* is one of the main etiological agents causing candidemia, just after *C. albicans*. Its prevalence has increased due to the development of antifungal resistance (8,9,24,57). Moreover, it possesses different virulence factors that make it a successful pathogen. Such is the case of high resistance to heat-shock, a strong response to oxidative stress, considerable genomic plasticity, and high adherence to medical devices and epithelial cells (11,58,59).

Identification of the etiological agent is crucial because each *Candida* spp. displays different antifungal susceptibility patterns and stress responses (60), even among strains from the same species or from strains that share a clonal origin (18). There are several methods to identify *Candida* spp., but culture methods remain the gold standard (20), nevertheless, methods with high specificity and sensitivity have been developed based on non-culture methods like PCR assays (2).

In this study, we emphasize the importance of characterizing *C. glabrata* contemporaneous strains (multiple index strains from one clinical sample at a specific time of the infection) to determine variability at genotypic and phenotypic levels. We identified 77 contemporaneous strains of *C. glabrata,* isolated from urine and blood clinical samples derived from 11 patients.

Contemporaneous clinical isolates from individual patients share a clonal origin

We confirmed the clonal origin of the 77 contemporaneous strains using three MLP molecular markers: *ERG3*, *RPM2*, and *MT-I*. These MLP markers have been used to genotype and determine the prevalence of some genotypes, and they can help to

562 determine genetic divergence among related or unrelated strains by identifying
563 alleles and genotypes from each clinical strain.
564 In our study, strains from blood samples were clustered into two genotypes.
565 Strains from P6 and P13 are clustered in genotype I, whereas those from P8 are in
566 genotype II (Figure 1B). In addition, strains from urine samples were clustered into
567 six genotypes (Figure 1C). Genotypes I and V were more frequent because each
568 genotype groups isolates from two patients (genotype I: P17 and P21, whereas
569 genotype V: P18 and P22). Genotypes II, III, IV, and VI group strains from P23, P16,
570 P19, and P20, respectively. Genotype I was the most frequent in the strains from
571 blood and urine cultures.
572 Even though these genotyping methods are used to identify the genetic
573 diversity or genetic relationship among strains, in our study, we did not find major
574 differences among contemporaneous isolates from P6, P17, and P18, when we used
575 RAPD and *EPA1* microsatellites, but we found differences with MLP markers,
576 suggesting that a method with a greater resolution is needed, such as WGS.
577 However, our results suggest that the strains from each patient share a clonal origin.
578
579 **There is phenotypic variability among contemporaneous *C. glabrata* clinical**
580 **isolates**
581 Throughout an infection, identification and characterization of *C. glabrata,* as well as
582 other pathogens, consists of collecting and characterizing an index strain from the
583 clinical sample, and a treatment is offered to the patient. This methodology is based
584 on IAH, which states that a single organism is the cause of the infection, and it has
585 been well studied in sequential clinical isolates, observing the pathogen adaptation
586 over time to different conditions (microevolution process). (14,15,17). Recently,
587 multiple index strains were collected at the beginning of the infection with *C. glabrata*
588 (contemporaneous strains), and variability at phenotypic and genotypic levels was
589 found (18). Similar results were obtained with pathogenic prokaryotic *Klebsiella*
590 *pneumoniae* carbapenem-resistant (19).
591 In this study, we characterized the response of *C. glabrata* contemporaneous
592 strains from blood and urine clinical samples to different stresses to determine

whether there is phenotypic variability among contemporaneous isolates. We not only characterized the response to antifungals, but also the response to heat-shock, oxidative stress, and cell-wall perturbing agents, which have not been documented in contemporaneous strains. As expected, we found a variety of phenotypes among strains from 11 patients, but only strains derived from three patients displayed phenotypic variability among their corresponding contemporaneous strains: P6 (blood culture), P17 (urine culture), and P18 (urine culture) (Supplementary Figures S4 and S5).

Interestingly, SL357, SL345, SL385, SL347, and SL348, which are FLC^R, showed caffeine resistance. Caffeine in yeast has been described as a cell wall perturbing agent, but also drives pleiotropic effects (41). Mechanisms by which *C. glabrata* can be resistant to caffeine have not been defined yet. Still, in *Saccharomyces cerevisiae*, the *SNQ2* gene (which encodes an efflux pump) has been documented to confer resistance to caffeine. Moreover, the *PDR1* gene can increase the expression of ABC-transporter-encoding genes *CDR1, CDR2*, and *SNQ2* in FLC^R *C. glabrata* (49). Therefore, this suggests that the ABC-transporters may play a role in caffeine resistance in these strains.

These data show that phenotypic variability is present in contemporaneous strains from both blood and urine clinical samples, and these differences are not only limited to antifungal resistance, but also stress responses, which are important traits to successfully infect a susceptible host. In addition, recovering and characterizing multiple cotemporaneous index strains during infection is highly recommended to avoid an underestimation of susceptibility profiles for etiological agents.

Hassoun *et al*., (2024) demonstrated that the gut could be a reservoir for the emergence of mutations related to echinocandin resistance before and after CSP therapy by a mouse infection model with *C. glabrata*. Therefore, genotypic variability before treatment with antifungals or antibiotics may occur, leading to phenotypic variability of the pathogen. Under selective pressure, such as treatment with antifungals, resistance can be acquired or selected, leading to persistent infections. This could be an explanation for this variability at the beginning of infection, however, because clinical history is not available for the patients in this study, it is difficult to

know if this variability may have previously existed or emerged after antifungal treatment.

Some clinical samples contain a mixture of Gly+ and Gly- (petite) strains

Four strains from P17 exhibit a petite phenotype under non-fermentable carbon sources characterization (YPG) (Supplementary Figure S6A). However, SL345, SL346, and SL348 showed growth in YPG media in posterior analysis (Figure 7B and Supplementary Figure S6A). This could be due to either a switch between cells that have functional mitochondria (Gly+) and cells with dysfunctional mitochondria (Gly-), or a contamination of a mainly Gly- strain with some Gly+ cells of the same strain. We performed an assay with these petite strains to determine the proportion of Gly+ and Gly- in 10 independent cultures, and replica plating in YPD and YPG. Surprisingly, SL345, SL346, and SL347 showed NCVs and SCVs in YPD. However, these NCVs did not appear in all the plates tested, unlike SCVs, which appeared in all plates tested (Tables 3-7). Only NCVs were able to grow in YPG in the replica plate (Gly+ phenotype) (Supplementary Figure S6B). SL346 was the first strain that showed this phenomenon, and we purified the strain to obtain Gly+ and Gly- strains which we kept separately as SL384 and SL385, respectively for further analysis. Interestingly, SL384 (Gly+), which comes from a petite strain, is not resistant to FLC or caffeine. Instead, it showed a similar phenotype to SL322 and SL339 Gly+ strains (Figures 2-7). Our MitoTracker™ Green FM staining is consistent with the ability of each strain to use non-fermentable carbon sources like glycerol: Gly- strains showed a diffuse staining and no clear mitochondria or mitochondrial network, while Gly+ strains display intense mitochondria and a defined network (Figure 8).

So far, we cannot conclude that these strains are undergoing a reversion process from Gly- to Gly+ phenotype *in vitro* or whether the strains are, in fact, a mixed population of Gly- with Gly+ cells from the original clinical sample. We need to further analyze the strains separately to determine whether this is a reversion or a switch process similar to what has been found when *C. glabrata* is phagocytosed by macrophages where it switches to a petite phenotype, improving its fitness to

survive in immune cells, when there is no selective pressure, it can switch back to a Gly+ phenotype (62).

The Gly+ FLC^R strain SL357 does not have a GOF mutation in *PDR1*

During candidiasis, FLC has been the first-line antifungal, and prolonged exposure leads to a propensity to acquire an FLC^R (63,64). Fluconazole binds to the lanosterol demethylase enzyme (encoded by the *ERG11* gene), which participates in ergosterol biosynthesis; therefore, this binding inhibits ergosterol biosynthesis and leads to an accumulation of toxic sterols. However, resistance to fluconazole is frequently observed, and it is mediated by different mechanisms like alterations in the drug target (*ERG11*) as well as GOF mutations in the *PDR1* gene, which encodes the transcription factor Pdr1, which can induce the transcription of the main drug efflux pumps; consequently, an overexpression of the drug efflux pumps leads to FLC resistance (50,65,66). Another mechanism by which *C. glabrata* can acquire resistance to fluconazole is mitochondrial dysfunction (petite phenotype); nevertheless, this only mediates an overexpression of the *PDR1* gene (42,43).

Contemporaneous strain SL357 from P18, which is Gly+, and SL385, which is Gly- (purified strain from SL346 derived from P17), are FLC^R (Figure 2), and we decided to sequence the *PDR1* gene to determine if there are GOF mutations. We found S76P and T143P polymorphisms in Pdr1 of SL357 and SL385, compared to the reference strains. However, these alleles are not located in any previously described domain, but they are between the DNA-binding domain (BD) and the Middle Homology domain (MHD) (52). Both polymorphisms usually appear together and are present in many clinical isolates regardless of whether they are sensitive or resistant to FLC. Therefore, these are not considered GOF mutations (14,51,53,67).

Therefore, the FLC resistance phenotypes of SL357 and SL385 are not due to mutations in Pdr1. In the case of SL357, other mechanisms could confer the low susceptibility to FLC. For instance, Upc2A is a transcription factor involved in ergosterol biosynthesis that regulates the expression of *ERG* genes, but it has also been reported that an overexpression of the *UPC2A* gene by low ergosterol levels,

684 leads to a higher transcription of Upc2a and binding to genes involved in FLC
685 resistance, such as *CDR1*, *PDR1* and *ERG11* (68,69).

686 Finally, it is important to highlight the proportion of phenotypic and genotypic
687 variability in contemporaneous strains. In a similar study, researchers discovered
688 variability among *C. glabrata* contemporaneous strains in strains derived from 2 of
689 10 patients studied, emphasizing antifungal resistance (18). We found that isolates
690 from 3 of 11 patients were identified with phenotypic variability to different stresses.
691 Therefore, about 20% of patients may be infected by mixed populations of clonal *C.*
692 *glabrata* cells that display phenotypic and genotypic variability, some of which can
693 confer resistance to antifungals and may remain undetected. This is very important
694 to consider as it could result in failed treatments for some patients. Ideally, clinical
695 laboratories should characterize at least 5 index strains before administering the
696 treatment.

Conclusion

We identified 77 contemporaneous strains of *C glabrata* from blood and urine clinical samples from 11 patients; all contemporaneous strains from individual patients shared a clonal origin using 3 different markers. However, a method with high resolution, like WGS, will be necessary to identify genomic differences among patients.

Isolates from three patients (P6, P17, and P18) exhibited significant phenotypic differences, not only in antifungal response but also under other stresses. Likewise, the presence of variability in 3 of 11 patients indicates that it is an important proportion in the population in clinical settings. Nevertheless, collecting more than one index strain from the beginning and during the infection can allow technicians to identify such variability and avoid therapy failures, thereby enriching the resistant population.

We cannot determine if the four petite, P17-derived strains can switch from a state of functional to dysfunctional mitochondria, or reversion from Gly- to Gly+ phenotype, or a mixed population of Gly- and Gly+ cells from the original sample. Further assays will be necessary to identify the mechanism that is responsible for this phenomenon.

The *PDR1* gene exhibits several nucleotide variations, however, many of them were synonymous changes. Polymorphisms S76P and T143P present in the petite SL385 and Gly+ SL357 are not involved in FLC-resistance and other mechanisms; possibly *UPC2A* could be responsible for the FLC^R phenotype.

Perspectives

Contemporaneous strains from P17 and P18 are of particular interest due to the phenotypic variability presented.

To further characterize the Gly- phenotype from the four petite strains belonging to P17, we will perform the following experiments:

1. To isolate Gly- and Gly+ strains from the SL345, SL347, and SL348 clinical isolates by colony purification.
2. To determine if there are reversion processes in Gly- and Gly+ strains by passes in YPD rich media without selection pressure (FLC).
3. To quantify the mitochondrial DNA from Gly- and Gly+ strains by qPCR with *COX2* and *COX3* mitochondrial genes.
4. To determine the genetic relatedness of some Gly+ and Gly- strains by WGS of selected isolates.
5. To determine the presence of mitochondria in Gly- and Gly+ strains with a plasmid containing a specific mitochondrial protein (*PRX1)* tagged with GFP.
6. To determine the Minimum Inhibitory Concentration (MIC) of Gly- and Gly+ strains against antifungals.

On the other hand, to further characterize the P18-derived strains and the mechanisms that could confer resistance to SL357 (FLC^R), we will:

1. Determine the Minimum Inhibitory Concentration (MIC) of the strains against antifungals.
2. Measure the expression levels of genes involved in FLC and CSP resistance by RT-qPCR.
3. Determine if there are mutations in *UPC2A* that confer the FLC^R phenotype.
4. Construct a single mutant *upc2a*Δ in the SL357 strain to compare its phenotype with the FLC^R phenotype of the contemporaneous isolates.
5. Perform a ChIP-qPCR to determine if Upc2a is activating *PDR1* and *CDR1.*
6. To determine the clonal origin and mutations in other genes involved in FLC^R by WGS of selected isolates.

748 Likewise, we will assess whether there are differences in infection fitness. To
749 achieve this, we will challenge the strains *in vitro* against neutrophils and
750 macrophages. In addition, we will measure the mortality rates of the strains
751 infecting *Galleria mellonella* larvae.

References

1. Fisher MC, Alastruey-Izquierdo A, Berman J, Bicanic T, Bignell EM, Bowyer P, et al. Tackling the emerging threat of antifungal resistance to human health. Nat Rev Microbiol. 2022;20(9):557–71.
2. Clancy CJ, Nguyen MH. Diagnosing invasive candidiasis. J Clin Microbiol. 2018;56(5):1–9.
3. Miller JM, Binnicker MJ, Campbell S, Carroll KC, Chapin KC, Gilligan PH, et al. A Guide to Utilization of the Microbiology Laboratory for Diagnosis of Infectious Diseases: 2018 Update by the Infectious Diseases Society of America and the American Society for Microbiology. Clin Infect Dis. 2018;67(6):813–6.
4. McCarty TP, White CM, Pappas PG. Candidemia and Invasive Candidiasis. Infect Dis Clin North Am [Internet]. 2021;35(2):389–413. Available from: https://doi.org/10.1016/j.idc.2021.03.007
5. Cauchie M, Desmet S, Lagrou K. Candida and its dual lifestyle as a commensal and a pathogen. Res Microbiol [Internet]. 2017;168(9–10):802–10. Available from: https://doi.org/10.1016/j.resmic.2017.02.005
6. Mba IE, Nweze EI. Mechanism of Candida pathogenesis: revisiting the vital drivers. Eur J Clin Microbiol Infect Dis. 2020;39(10):1797–819.
7. WHO. WHO fungal priority pathogens list to guide research, development and public health action. Vol. 1, Licence: CC BY-NC-SA 3.0 IGO. 2022. 1–48 p.
8. Diekema D, Arbefeville S, Boyken L, Kroeger J, Pfaller M. The changing epidemiology of healthcare-associated candidemia over three decades. Diagn Microbiol Infect Dis [Internet]. 2012;73(1):45–8. Available from: http://dx.doi.org/10.1016/j.diagmicrobio.2012.02.001
9. Pfaller MA, Andes DR, Diekema DJ, Horn DL, Reboli AC, Rotstein C, et al. Epidemiology and outcomes of invasive candidiasis due to non-albicans species of Candida in 2,496 patients: Data from the Prospective Antifungal Therapy (PATH) registry 2004-2008. PLoS One. 2014;9(7).
10. Naicker SD, Shuping L, Zulu TG, Mpembe RS, Mhlanga M, Tsotetsi EM, et al. Epidemiology and susceptibility of Nakaseomyces (formerly Candida) glabrata bloodstream isolates from hospitalised adults in South Africa. Med Mycol. 2023;61(6):15–7.
11. López-Fuentes E, Gutiérrez-Escobedo G, Timmermans B, Dijck P Van, Peñas AD Las, Castaño I. Candida glabrata's genome plasticity confers a unique pattern of expressed cell wall proteins. J Fungi. 2018;4(2).
12. Brooks GF, Carroll KC, Butel JS, Morse SA, Mietzner TA. Medical Microbiology. 25a ed. McGRAW-HILL INTERAMERICANA EDITORES SA de CV, editor. Mexico D.F.: The McGraw-Hill; 2016.
13. Rubin LG. Bacterial colonization and infection resulting from multiplication of a single organism. Rev Infect Dis. 1987;9(3):488–93.
14. Carreté L, Ksiezopolska E, Gómez-Molero E, Angoulvant A, Bader O, Fairhead C, et al. Genome comparisons of Candida glabrata serial clinical isolates reveal patterns of genetic variation in infecting clonal populations.

Front Microbiol. 2019;10(FEB):1–13.
15. Misas E, Seagle E, Jenkins EN, Rajeev M, Hurst S, Nunnally NS, et al. Erratum for Misas et al., “Genomic description of acquired fluconazole- and echinocandin-resistance in patients with serial Candida glabrata isolates.” J Clin Microbiol. 2024;62(6):e0060824.
16. Stefanini I, Stoakes E, Wu HHT, Xu-McCrae L, Hussain A, Moat J, et al. Genomic Assembly of Clinical Candida glabrata (Nakaseomyces glabrata) Isolates Reveals within-Species Structural Plasticity and Association with In Vitro Antifungal Susceptibility . Microbiol Spectr. 2022;10(6):1–14.
17. López-Marmolejo AL, Hernández-Chávez MJ, Gutiérrez-Escobedo G, Selene Herrera-Basurto M, Mora-Montes HM, De Las Peñas A, et al. Microevolution of Candida glabrata (Nakaseomyces glabrata) during an infection. Fungal Genet Biol. 2024;172(March).
18. Badrane H, Cheng S, Dupont CL, Hao B, Driscoll E, Morder K, et al. Genotypic diversity and unrecognized antifungal resistance among populations of Candida glabrata from positive blood cultures. Nat Commun. 2023;14(1).
19. Cheng S, Fleres G, Chen L, Liu G, Hao B, Newbrough A, et al. Within-Host Genotypic and Phenotypic Diversity of Contemporaneous Carbapenem-Resistant Klebsiella pneumoniae from Blood Cultures of Patients with Bacteremia. MBio. 2022;13(6).
20. Hernández-Carreón O, Hernández-Howell C, Hernández-Hernández G, Herrera-Basurto MS, González-Gómez BE, Gutiérrez-Escobedo G, et al. Highly specific and rapid molecular detection of Candida glabrata in clinical samples. Brazilian J Microbiol [Internet]. 2021;52(4):1733–44. Available from: https://doi.org/10.1007/s42770-021-00584-2
21. Foulet F, Nicolas N, Eloy O, Botterel F, Gantier JC, Costa JM, et al. Microsatellite marker analysis as a typing system for Candida glabrata. J Clin Microbiol. 2005;43(9):4574–9.
22. López Marmolejo AL, Castaño Navarro IB, Gutiérrez Escobedo MG. Análisis fenotípico y genotípico de aislados clinicos secuenciales de C. glabrata. 2021.
23. Selene M, Basurto H, Irene D, Castaño B, Ma D, Gutiérrez G. Caracterización molecular y fenotípica de aislados clínicos secuenciales de Candida glabrata pertenecientes a un mismo paciente. 2020;
24. Parslow BY, Thornton CR. Continuing Shifts in Epidemiology and Antifungal Susceptibility Highlight the Need for Improved Disease Management of Invasive Candidiasis. Microorganisms. 2022;10(6).
25. Kumar K, Askari F, Sahu MS, Kaur R. Candida glabrata: A lot more than meets the eye. Microorganisms. 2019;7(2):1–22.
26. Katsipoulaki M, Stappers MHT, Malavia-jones D, Brunke S, Hube B, Gow NAR. Priority Pathogens. Vol. 0, Microbiology and Molecular Biology Reviews. American Society for Microbiology; 2024. 1–45 p.
27. Ferngren G, Yu D, Unalan-Altintop T, Dinnétz P, Özenci V. Epidemiological patterns of candidaemia: A comprehensive analysis over a decade. Mycoses. 2024;67(5):1–7.
28. Gülmez D, Alp S, Gursoy G, Ayaz CM, Dogan O, Arikan-Akdagli S, et al.

Mixed fungaemia: an 18-year report from a tertiary-care university hospital and a systematic review. Clin Microbiol Infect [Internet]. 2020;26(7):833–41. Available from: https://doi.org/10.1016/j.cmi.2020.03.030
29. Tumbarello M, Fiori B, Trecarichi EM, Posteraro P, Losito AR, de Luca A, et al. Invasive fungal infections in patients with cancer in the Intensive Care Unit. PLoS One [Internet]. 2012;56(3):264–72. Available from: http://dx.doi.org/10.1016/j.ijantimicag.2011.11.017
30. Sipsas N V., Kontoyiannis DP. Invasive fungal infections in patients with cancer in the Intensive Care Unit. Int J Antimicrob Agents [Internet]. 2012;39(6):464–71. Available from: http://dx.doi.org/10.1016/j.ijantimicag.2011.11.017
31. Li WS, Chen YC, Kuo SF, Chen FJ, Lee CH. The impact of biofilm formation on the persistence of candidemia. Front Microbiol. 2018;9(JUN):1–10.
32. Pannanusorn S, Fernandez V, Römling U. Prevalence of biofilm formation in clinical isolates of Candida species causing bloodstream infection. Mycoses. 2013;56(3):264–72.
33. Abbes S, Amouri I, Sellami H, Sellami A, Makni F, Ayadi A. A review of molecular techniques to type Candida glabrata isolates. Mycoses. 2010;53(6):463–7.
34. Marol S, Yücesoy M. Molecular epidemiology of Candida species isolated from clinical specimens of intensive care unit patients. Mycoses. 2008;51(1):40–9.
35. Bonatti H, Stelzmueller I, Berger N, Lechner M, Grif K, Geltner C, et al. Infections caused by candida krusei in five transplant and two surgical patients. Surg Infect (Larchmt). 2009;10(3):265–71.
36. Raposo CJ, McElroy KA, Fuchs SM. The Epithelial adhesin 1 tandem repeat region mediates protein display through multiple mechanisms. FEMS Yeast Res. 2020;20(3):1–9.
37. Cormack BP, Ghori N, Falkow S. An adhesin of the yeast pathogen Candida glabrata mediating adherence to human epithelial cells. Science (80-). 1999;285(5427):578–82.
38. Frías-De-león MG, Hernández-Castro R, Conde-Cuevas E, García-Coronel IH, Vázquez-Aceituno VA, Soriano-Ursúa MA, et al. Candida glabrata antifungal resistance and virulence factors, a perfect pathogenic combination. Pharmaceutics. 2021;13(10).
39. Pais P, Galocha M, Viana R, Cavalheiro M, Pereira D, Teixeira MC. Microevolution of the pathogenic yeasts Candida albicans and Candida glabrata during antifungal therapy and host infection. Microb Cell. 2019;6(3):142–59.
40. Hassan Y, Chew SY, Than LTL. Candida glabrata: Pathogenicity and resistance mechanisms for adaptation and survival. J Fungi. 2021;7(8).
41. Chung WH. Pleiotropic effects of caffeine leading to chromosome instability and cytotoxicity in eukaryotic microorganisms. J Microbiol Biotechnol. 2021;31(2):171–80.
42. Tsai HF, Krol AA, Sarti KE, Bennett JE. Candida glabrata PDR1, a transcriptional regulator of a pleiotropic drug resistance network, mediates azole resistance in clinical isolates and petite mutants. Antimicrob Agents

Chemother. 2006;50(4):1384–92.
43. Ferrari S, Sanguinetti M, De Bernardis F, Torelli R, Posteraro B, Vandeputte P, et al. Loss of mitochondrial functions associated with azole resistance in Candida glabrata results in enhanced virulence in mice. Antimicrob Agents Chemother. 2011;55(5):1852–60.
44. Brun S, Bergés T, Poupard P, Vauzelle-Moreau C, Renier G, Chabasse D, et al. Mechanisms of Azole Resistance in Petite Mutants of Candida glabrata. Antimicrob Agents Chemother. 2004;48(5):1788–96.
45. Brun S, Dalle F, Saulnier P, Renier G, Bonnin A, Chabasse D, et al. Biological consequences of petite mutations in Candida glabrata. J Antimicrob Chemother. 2005;56(2):307–14.
46. Arastehfar A, Daneshnia F, Hovhannisyan H, Fuentes D, Cabrera N, Quinteros C, et al. vivo fitness. 2023;14(5).
47. Neikirk K, Marshall AG, Kula B, Smith N, LeBlanc S, Hinton A. MitoTracker: A useful tool in need of better alternatives. Eur J Cell Biol [Internet]. 2023;102(4):151371. Available from: https://doi.org/10.1016/j.ejcb.2023.151371
48. Pappas PG, Lionakis MS, Arendrup MC, Ostrosky-Zeichner L, Kullberg BJ. Invasive candidiasis. Nat Rev Dis Prim [Internet]. 2018;4(May):1–20. Available from: http://dx.doi.org/10.1038/nrdp.2018.26
49. Sanguinetti M, Posteraro B, Fiori B, Ranno S, Torelli R, Fadda G. Mechanisms of azole resistance in clinical isolates of Candida glabrata collected during a hospital survey of antifungal resistance. Antimicrob Agents Chemother. 2005;49(2):668–79.
50. Ferrari S, Sanguinetti M, Torelli R, Posteraro B, Sanglard D. Contribution of CgPDR1-regulated genes in enhanced virulence of azole-resistant Candida glabrata. PLoS One. 2011;6(3).
51. Ferrari S, Ischer F, Calabrese D, Posteraro B, Sanguinetti M, Fadda G, et al. Gain of function mutations in CgPDR1 of Candida glabrata not only mediate antifungal resistance but also enhance virulence. PLoS Pathog. 2009;5(1).
52. Arastehfar A, Daneshnia F, Salehi M, Yaşar M, Hoşbul T, Ilkit M, et al. Low level of antifungal resistance of Candida glabrata blood isolates in Turkey: Fluconazole minimum inhibitory concentration and FKS mutations can predict therapeutic failure. Mycoses. 2020;63(9):911–20.
53. Fattouh N, Khalaf RA, Husni R. Candida glabrata hospital isolate from Lebanon reveals micafungin resistance associated with increased chitin and resistance to a cell-surface-disrupting agent. J Glob Antimicrob Resist. 2024;37:62–8.
54. Ni Q, Wang C, Tian Y, Dong D, Jiang C, Mao E, et al. CgPDR1 gain-of-function mutations lead to azole-resistance and increased adhesion in clinical Candida glabrata strains. Mycoses. 2018;61(7):430–40.
55. Brown GD, Denning DW, Gow NAR, Levitz SM, Netea MG, White TC. Hidden killers: Human fungal infections. Sci Transl Med. 2012;4(165):1–10.
56. Bongomin F, Gago S, Oladele RO, Denning DW. Global and multi-national prevalence of fungal diseases—estimate precision. J Fungi. 2017;3(4).
57. White MH. Editorial Response : The Contribution of Fluconazole to the Changing Epidemiology of Invasive Candidal Infections. :1129–30.

58. Cuéllar-Cruz M, Briones-Martin-del-Campo M, Cañas-Villamar I, Montalvo-Arredondo J, Riego-Ruiz L, Castaño I, et al. High resistance to oxidative stress in the fungal pathogen Candida glabrata is mediated by a single catalase, Cta1p, and is controlled by the transcription factors Yap1p, Skn7p, Msn2p, and Msn4p. Eukaryot Cell. 2008;7(5):814–25.
59. Lim SJ, Mohamad Ali MS, Sabri S, Muhd Noor ND, Salleh AB, Oslan SN. Opportunistic yeast pathogen Candida spp.: Secreted and membrane-bound virulence factors. Med Mycol. 2021;59(12):1127–44.
60. Pote ST, Sonawane MS, Rahi P, Shah SR, Shouche YS, Patole MS, et al. Distribution of pathogenic yeasts in different clinical samples: Their identification, antifungal susceptibility pattern, and cell invasion assays. Infect Drug Resist. 2020;13:1133–45.
61. Hassoun Y, Aptekmann AA, Keniya M V, Gomez RY, Alayo N, Novi G, et al. Evolutionary dynamics in gut-colonizing Candida glabrata during caspofungin therapy : Emergence of clinically important mutations in sphingolipid biosynthesis. 2024;1–25. Available from: http://dx.doi.org/10.1371/journal.ppat.1012521
62. Siscar-Lewin S, Gabaldón T, Aldejohann AM, Kurzai O, Hube B, Brunke S. Transient mitochondria dysfunction confers fungal cross-resistance against phagocytic killing and fluconazole. MBio. 2021;12(3).
63. Goemaere B, Lagrou K, Spriet I, Hendrickx M. Clonal Spread of Candida glabrata Bloodstream Isolates and Fluconazole Resistance Affected by Prolonged Exposure : a 12-. 2018;
64. Pappas PG, Rex JH, Sobel JD, Filler SG, Dismukes WE, Walsh TJ, et al. Guidelines for treatment of candidiasis. Infect Dis Clin Pract. 2004;12(4):245–6.
65. Vermitsky JP, Edlind TD. Azole resistance in Candida glabrata: Coordinate upregulation of multidrug transporters and evidence for a Pdr1-like transcription factor. Antimicrob Agents Chemother. 2004;48(10):3773–81.
66. Robbins N, Cowen LE. Antifungal drug resistance: Deciphering the mechanisms governing multidrug resistance in the fungal pathogen Candida glabrata. Curr Biol [Internet]. 2021;31(23):R1520–3. Available from: https://doi.org/10.1016/j.cub.2021.09.071
67. Merdan O, Şişman AS, Aksoy SA, Kızıl S, Tüzemen NÜ, Yılmaz E, et al. Investigation of the Defective Growth Pattern and Multidrug Resistance in a Clinical Isolate of Candida glabrata Using Whole-Genome Sequencing and Computational Biology Applications. Microbiol Spectr. 2022;10(4).
68. Vu BG, Stamnes MA, Li Y, David Rogers P, Scott Moye-Rowley W. The Candida glabrata Upc2A transcription factor is a global regulator of antifungal drug resistance pathways. PLoS Genet [Internet]. 2021;17(9):1–27. Available from: http://dx.doi.org/10.1371/journal.pgen.1009582
69. Vu BG, Moye-Rowley WS. Nonidentical function of Upc2A binding sites in the Candida glabrata CDR1 promoter. Genetics. 2022;222(2):1–11.

Tables

Table 1. Clinical samples, data, and results of identification and clonality of 77 *Candida glabrata* contemporaneous strains.

Origin	Patient	Clinical sample	Date	Contemp. strains	*C. glabrata* identification			Clonality		
					Cg 1	Cg 2	Cg 3	ERG3	MT-I	RPM2
Blood	Patient 6	AN365	March 22, 2014	AN787	✔	✔	✔	CLONAL		
				AN788	✔	✔	✔			
				AN789	✔	✔	✔			
				AN790	✔	✔	✔			
				AN791	✔	✔	✔			
		AN366	March 22, 2014	AN792	✔	✔	✔	CLONAL		
				AN793	✔	✔	✔			
				AN794	✔	✔	✔			
				AN795	✔	✔	✔			
				AN796	✔	✔	✔			
	Patient 8	AN508	Feb. 17, 2016	AN797	✔	✔	✔	CLONAL		
				AN798	✔	✔	✔			
				AN799	✔	✔	✔			
				AN800	✔	✔	✔			
				AN801	✔	✔	✔			
		AN509		AN802	✔	✔	✔	CLONAL		

			Feb. 17, 2016	AN803	✔	✔	✔	
				AN804	✔	✔	✔	
				AN805	✔	✔	✔	
				AN806	✔	✔	✔	
		AN510	Feb. 17, 2016	AN807	✔	✔	✔	CLONAL
				AN808	✔	✔	✔	
				AN809	✔	✔	✔	
				AN810	✔	✔	✔	
				AN811	✔	✔	✔	
	Patient 13	AN239	Dec. 13, 2013	AN777	✔	✔	✔	CLONAL
				AN778	✔	✔	✔	
				AN779	✔	✔	✔	
				AN780	✔	✔	✔	
				AN781	✔	✔	✔	
		AN240	Dec 13, 2013	AN782	✔	✔	✔	CLONAL
				AN783	✔	✔	✔	
				AN784	✔	✔	✔	
				AN785	✔	✔	✔	
				AN786	✔	✔	✔	
Urine	Patient 16	SL143	Nov. 30, 2013	SL325	✔	✔	✔	CLONAL
				SL349	✔	✔	✔	
				SL350	✔	✔	✔	
				SL351	✔	✔	✔	
				SL352	✔	✔	✔	

				SL353	✔	✔	✔	
	Patient 17	SL309	May 26, 2013	SL322	✔	✔	✔	CLONAL
				SL339	✔	✔	✔	
				SL345	✔	✔	✔	
				SL346	✔	✔	✔	
				SL347	✔	✔	✔	
				SL348	✔	✔	✔	
	Patient 18	SL129	Sep. 26, 2013	SL354	✔	✔	✔	CLONAL
				SL355	✔	✔	✔	
				SL356	✔	✔	✔	
				SL357	✔	✔	✔	
				SL358	✔	✔	✔	
	Patient 19	SL152	Nov. 21, 2013	SL364	✔	✔	✔	CLONAL
				SL365	✔	✔	✔	
				SL366	✔	✔	✔	
				SL367	✔	✔	✔	
				SL368	✔	✔	✔	
	Patient 20	SL157	Nov. 21, 2013	SL359	✔	✔	✔	CLONAL
				SL360	✔	✔	✔	
				SL361	✔	✔	✔	
				SL362	✔	✔	✔	
				SL363	✔	✔	✔	
	Patient 21	SL180		SL369	✔	✔	✔	CLONAL
				SL370	✔	✔	✔	

			Oct. 17, 2013	SL371	✔	✔	✔	
				SL372	✔	✔	✔	
				SL373	✔	✔	✔	
	Patient 22	SL202	Nov. 19, 2013	SL374	✔	✔	✔	CLONAL
				SL375	✔	✔	✔	
				SL376	✔	✔	✔	
				SL377	✔	✔	✔	
				SL378	✔	✔	✔	
	Patient 23	SL204	Nov. 19, 2013	SL379	✔	✔	✔	CLONAL
				SL380	✔	✔	✔	
				SL381	✔	✔	✔	
				SL382	✔	✔	✔	
				SL383	✔	✔	✔	

984

Table 2. Results of susceptibility assays under oxidative stress, heat shock, and two classes of antifungals.

Patient	Clinical sample	Contmep. Strains	Oxidative stress			Cell wall stress			Heat shock			Antifungals				
			H_2O_2 (mM)			Caffeine (mM)			Temperature (°C)			FLC. (µg/mL)			CSP. (µg/mL)	
			5	10	15	10	15	20	37	44	45	16	32	64	0.025	0.05
P 6	AN 365	AN 787														
		AN 788														
		AN 789														
		AN 790														
		AN 791														
	AN 366	AN 792														
		AN 793														
		AN 794														
		AN 795														
		AN 796														
P 8	AN 508	AN 797														
		AN 798														
		AN 799														
		AN 800														
		AN 801														
	AN 509	AN 802														
		AN 803														
		AN 804														
		AN 805														
		AN 806														
	AN 510	AN 807														
		AN 808														
		AN 809														
		AN 810														
		AN811														
P 13	AN 239	AN 777														
		AN 778														
		AN 779														
		AN 780														
		AN 781														

	AN 240	AN 782														
		AN 783														
		AN 784														
		AN 785														
		AN 786														
P 16	SL143	SL325														
		SL349														
		SL350														
		SL351														
		SL352														
		SL353														
P 17	SL309	SL322														
		SL339														
		SL345														
		SL346														
		SL347														
		SL348														
P 18	SL129	SL354														
		SL355														
		SL356														
		SL357														
		SL358														
P 19	SL152	SL364														
		SL365														
		SL366														
		SL367														
		SL368														
P 20	SL157	SL359														
		SL360														
		SL361														
		SL362														
		SL363														
P 21	SL180	SL369														
		SL370														
		SL371														
		SL372														

		SL373													
P 22	SL202	SL374													
		SL375													
		SL376													
		SL377													
		SL378													
P 23	SL204	SL379													
		SL380													
		SL381													
		SL382													
		SL383													

Red background means resistant, green background means susceptible.

Table 3. Gly+ and Gly- colonies obtained from the SL346 clinical isolate

Clinical isolate	Plates	Gly+ strains	Gly- strains	Total strains
SL346	**1**	-	**48**	**48**
	2	1	51	52
	3	-	70	70
	4	-	59	59
	5	-	52	52
	6	41	37	78
	7	14	52	66
	8	4	45	49
	9	-	35	35
	10	35	31	66
	10	**95**	**480**	**575**

Table 4. Gly+ and Gly- colonies obtained from the SL345 clinical isolate

G	Plates	Gly+ strains	Gly- strains	Total strains
SL345	**1**	-	44	44
	2	-	50	50
	3	-	49	49
	4	-	37	37
	5	21	30	51
	6	42	14	56
	7	8	33	41

	8	16	45	61
	9	11	51	62
	9	**98**	**353**	**451**

990 **Table 5. Gly+ and Gly- colonies obtained from the SL347 clinical isolate**

Clinical isolate	Plates	Gly+ strains	Gly- strains	Total strains
SL347	**1**	**10**	**16**	**26**
	2	-	37	37
	3	4	37	41
	4	-	44	44
	5	-	47	47
	6	-	44	44
	7	-	53	53
	8	-	37	37
	9	-	34	34
	10	-	44	44
	10	**14**	**393**	**407**

991 **Table 6. Gly+ and Gly- colonies obtained from the SL348 clinical isolate**

Clinical isolate	Plates	Gly+ strains	Gly- strains	Total strains
SL348	**1**	**-**	**40**	**40**
	2	-	44	44
	3	-	38	38
	4	-	45	45
	5	-	47	47
	6	-	63	63
	7	-	37	37
	8	-	40	40
	9	-	31	31
	10	-	56	56
	10	**-**	**441**	**441**

992

993 **Table 7. Gly+ and Gly- colonies obtained from the BG14 clinical isolate**

Clinical isolate	Plates	Gly+ strains	Gly- strains	Total strains
BG14	**1**	**61**	**-**	**61**
	2	45	-	45
	3	48	-	48
	4	43	1	44
	5	34	-	34
	6	52	1	53
	7	43	-	43
	8	34	-	34
	9	26	-	26
	10	37	-	37
	10	**423**	**2**	**425**

994

995

Table 8. List of primer sequences used to identify and to genotype contemporaneous clinical strains of *C. glabrata*

Primer	Sequence (5'-3')	Expected size (bp)
Cg1	Fw. CCA AAG TTC TAG TAT CTT ATT CTG TAT AAT	137 bp (Chr. K), 139 bp (Chr. E), 141 bp (Chr. H)
	Rv. GTG GAG TAG TTA GTT CTT GTG TCC AG	
Cg2	Fw. CGC TCA TAC AGG CAC AGA AG	324 bp (Chr. E), 348 bp (Chr. K), 364 bp (Chr. H)
	Rv. GTG GAG TAG TTA GTT CTT GTG TCC AG	
Cg3	Fw. GTG GAG TAG TTG GTA CTT GTG TCC	602 bp (Chr. C), 667 bp (Chr. C)
	Rv. ATA CCA CTC ATA TTC GTG CCA C	
RPM2	Fw. ATCTCCCAACTTCTCGTAGCC	Chromosome I (116-150 bp)
	Rv. ACTTGAACGACTTGAACGCC	
MT-I	Fw. CAGCAATAATAGCTTCTGACTATGAC	Chromosome D (227-251 bp)
	Rv. GACAGGAGCAACCGTTAGGA	
ERG3	Fw. AGTGCGAGTGTATGTAAAGAATG	Chromosome F (181-353 bp)
	Rv. CGTATACCTTATCTCCGTTCAA	
OPA-09	Fw. GGG TAA CGC C	Random fragments
OPA-18	Fw. AGC TGA CCG T	Random fragments
OPE-18	Fw. GGA CTG CAG A	Random fragments
EPA1 (INT) 2059	Fw. CGA CTT CAA TGC ATA CTT CCT CCG	800-1000 bp
EPA1 (INT) 2060	Rv. GGG TGC TAT GTA CCT TGC GAC ATG	
PDR1@ - 635 bp FW	Fw. TTACGTTCAAATTTTAAGTGGC	4749 bp
PDR1@789 bp RV	Rv. GGCAATGAATGTGGTGAAATAG	

Fw = Forward, Rv = Reverse. *Number of laboratory collection.

Table 9. List of *C. glabrata* control strains used in semi-quantitative growth-spot assay

Strains	Parental strain	Genotype	Phenotype
BG14 (CGM1)	BG2	*ura*3Δ*::Tn903* *Neo*^{R} Ura^{-}	Temperature-resistant (45°C)
*pdr1*Δ (CGM1094)	BG14	*ura*3Δ*::Tn903* G418^{R} *pdr1*Δ*::hph* Hyg^{R}	FLC-sensitive
*hst1*Δ (CGM84)	BG14	*ura*3Δ*::Tn903* G418^{R} *hst1*Δ*::ura3*	FLC-resistant
CBS138	WT	ATCC2001	Temperature-sensitive
*hdf1*Δ (CGM709)	BG14	*ura3*Δ*::Tn903* G418^{R} *hdf1*Δ*::hph* Hyg^{R}	Temperature-sensitive
*cta1*Δ (CGM392)	CGM295	ura3Δ::Tn903 G418^{R} *cta1*Δ::hph Hyg^{R} Ura^{-}	Oxidative stress-sensitive
*snq2*Δ (CGM5026)	BG14	*ura*3Δ*::Tn903* G418^{R} *snq2*Δ*::ura3* Ura^{+}	FLC-sensitive Caffeine-sensitive
AN376	WT	*FEN1* (Y220C)	CSP-resistant

Anexos

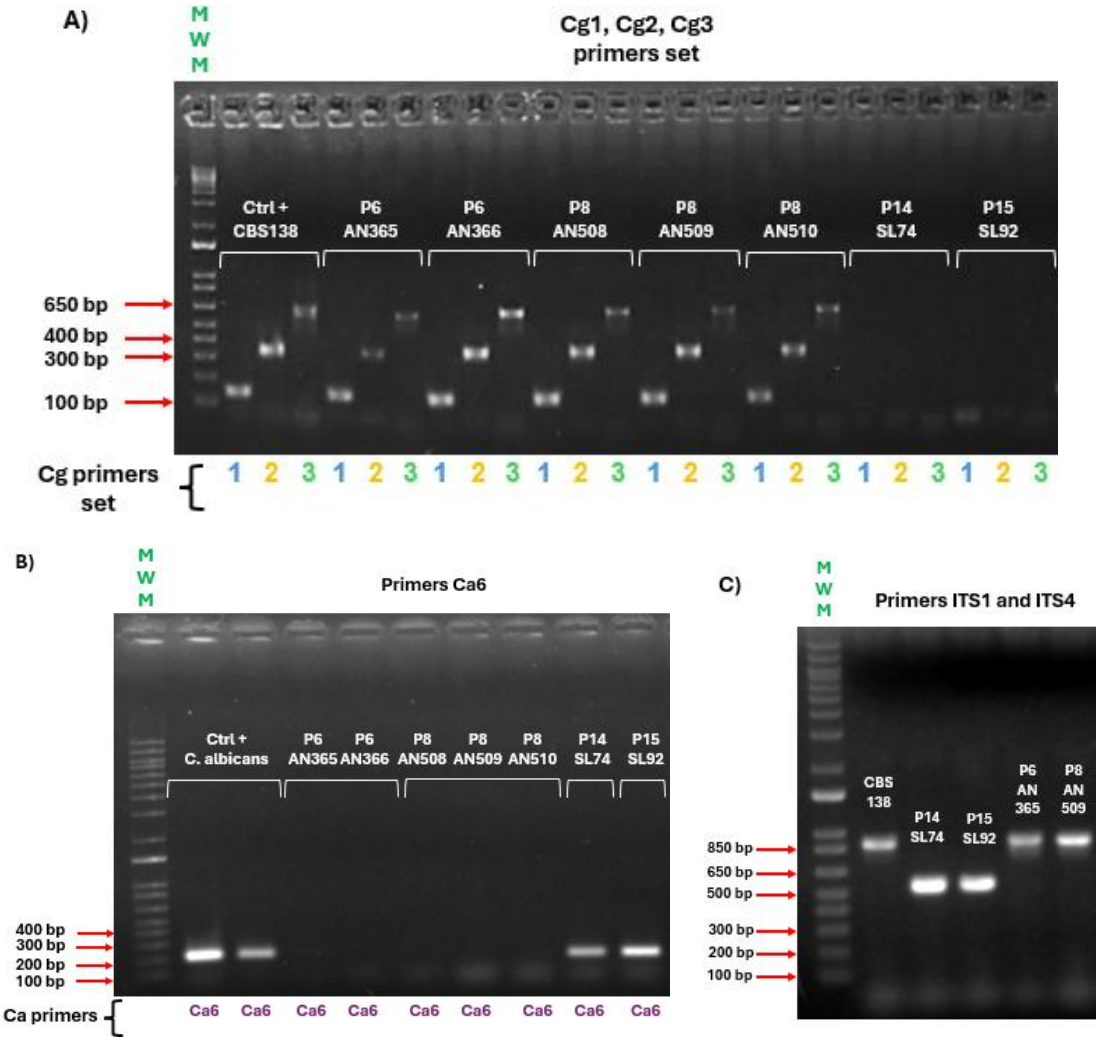

Supplementary Fig. S1. Identification of *C. glabrata* contemporaneous strains from clinical samples.

Cg1, Cg2, and Cg3 are a set of species-specific primers used to identify *C. glabrata* strains. Genomic DNA (gDNA) from blood and urine clinical samples was used as a template for end-point PCR using each primer set. **A)** P6 and P8 were identified as *C. glabrata* because we could amplify a PCR product of the expected size (similar to the positive control strain CBS138). Instead, P14 and P15 did not amplify with any of the primer sets. **B)** Clinical samples were diagnosed with *C. albicans*-specific oligonucleotides. Contemporaneous isolates from P6 and P8 did not amplify with the species-specific primers to *C. albicans*. However, P14 and P15 amplified a 200 bp expected product for this primer set (Ca6). Therefore, isolates from P14 and P15 are

C. albicans strains. **C)** The isolates from P14 and P15 amplify bands of the expected size for *C. albicans* by PCR with ITS primers. PCR product sizes from P14 and P15 were smaller compared with CBS138 and clinical samples from P6 and P8 previously identified as *C. glabrata*. The clinical samples from P14 and P15 amplify fragments of the expected size for *C. albicans* and not *C. glabrata*.

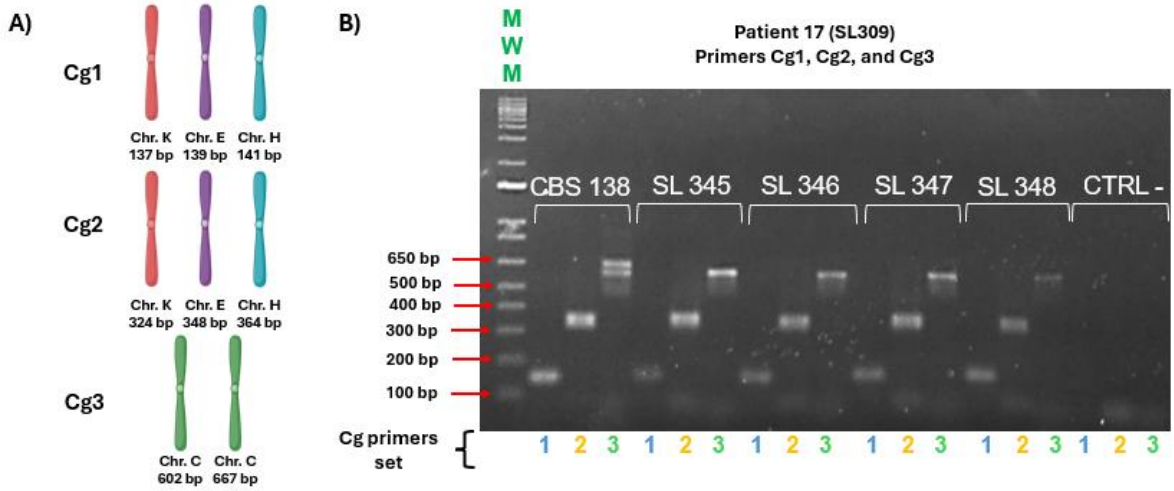

1020 **Supplementary Fig. S2. Identification of *C. glabrata* contemporaneous strains**
1021 **from P17.**

1022 **A)** Cg1, Cg2, and Cg3 are independent sets of primers used to identify *C. glabrata*
1023 strains, which amplify nearby regions to the *EPA1* gene in different chromosomes.
1024 PCR product sizes are shown for each set of primers. **B)** gDNA from four
1025 contemporaneous strains from a urine clinical sample from P17 (SL345 to SL348)
1026 was used as a template for end-point PCR using each primer set. The reference
1027 strain CBS138 was used as a positive control.

1028

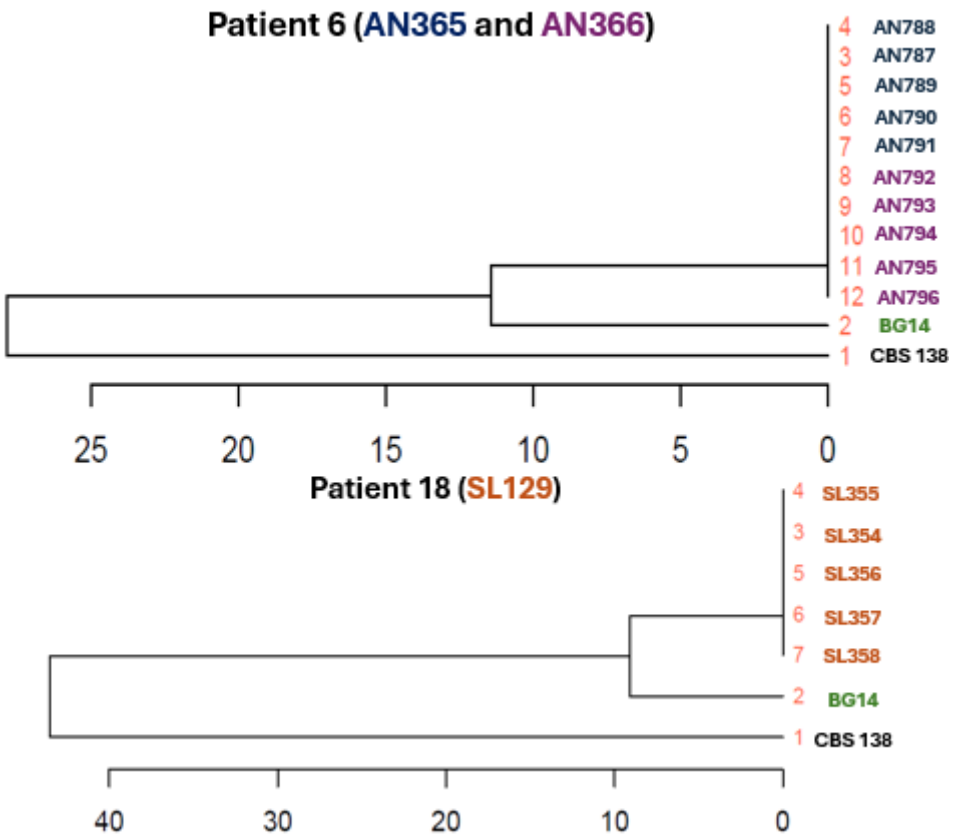

Supplementary Fig. S3. Dendrogram of *C. glabrata* contemporaneous strains from P6 and P18 by MLP markers.

ImageJ® and RStudio® were used to construct a dendrogram based on the sizes of PCR products obtained with each of the three molecular markers from strains of P6 and P18. The contemporaneous strains likely share a clonal origin because they were clustered together and separately from the reference strains.

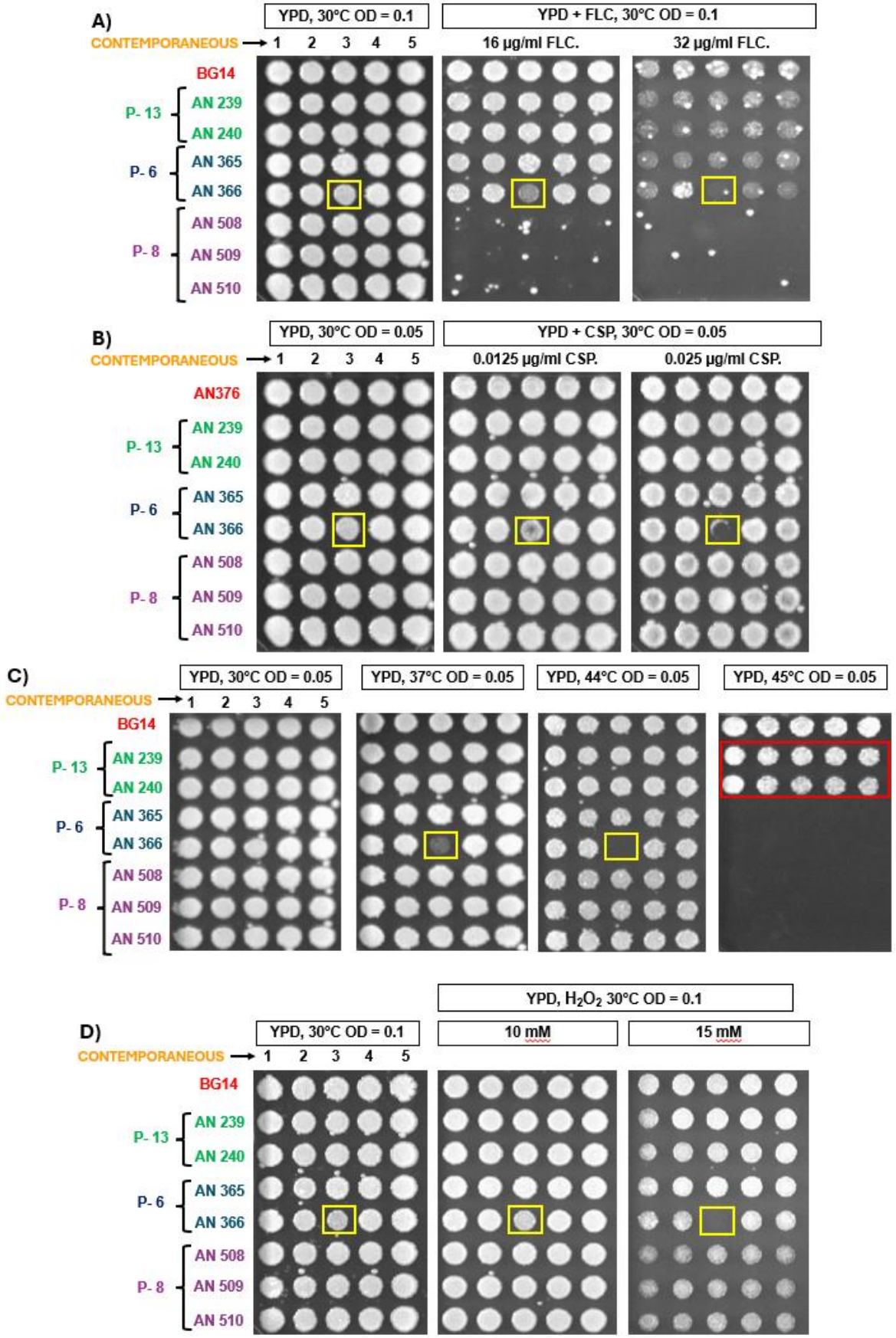
A)
YPD, 30°C OD = 0.1
YPD + FLC, 30°C OD = 0.1
CONTEMPORANEOUS
1 2 3 4 5
16 µg/ml FLC.
32 µg/ml FLC.
BG14
P- 13
AN 239
AN 240
P- 6
AN 365
AN 366
P- 8
AN 508
AN 509
AN 510
B)
YPD, 30°C OD = 0.05
YPD + CSP, 30°C OD = 0.05
CONTEMPORANEOUS
1 2 3 4 5
0.0125 µg/ml CSP.
0.025 µg/ml CSP.
AN376
P- 13
AN 239
AN 240
P- 6
AN 365
AN 366
P- 8
AN 508
AN 509
AN 510
C)
YPD, 30°C OD = 0.05
YPD, 37°C OD = 0.05
YPD, 44°C OD = 0.05
YPD, 45°C OD = 0.05
CONTEMPORANEOUS
1 2 3 4 5
BG14
P- 13
AN 239
AN 240
P- 6
AN 365
AN 366
P- 8
AN 508
AN 509
AN 510
D)
YPD, H2O2 30°C OD = 0.1
YPD, 30°C OD = 0.1
10 mM
15 mM
CONTEMPORANEOUS
1 2 3 4 5
BG14
P- 13
AN 239
AN 240
P- 6
AN 365
AN 366
P- 8
AN 508
AN 509
AN 510

Supplementary Fig. S4. Susceptibility assays of contemporaneous strains from blood cultures by drop-spot assay.

C. glabrata contemporaneous strains were adjusted at OD_{600} = 0.1 or 0.05 and then spotted on YPD plates at different concentrations of FLC (8, 16, 32, and 64 µg/mL), CSP (0.0125, 0.025, and 0.05 µg/mL), temperatures (30, 37, 44, and 45°C), and H_2O_2 (5, 10, and 15 mM). **A)** Strains from P6 and P13 show resistance to FLC at 16 µg/mL, except one contemporaneous strain from P6, AN366, which is FLC^S at 16 µg/mL (yellow square). All the strains from P8 are FLC^S at 16 µg/mL. **B)** One strain from P6 (AN366) is CSP^S at 0.025 µg/mL (yellow square), while their contemporaneous strains are resistant to CSP at this concentration. The contemporaneous strains derived from P8 and P13 are CSP^R to 0.025 µg/mL. **C)** One strain from P6, AN366, is sensitive at 37°C and 44°C (yellow square), whereas the rest of the strains from P6, and all strains from P8, and P13 are resistant at 44°C, and the strains from P13 are resistant at 45°C (red square). **D)** One strain from P6, AN366, is susceptible to 15 mM of H_2O_2 (yellow square), while its clonal contemporaneous strains can resist this concentration.

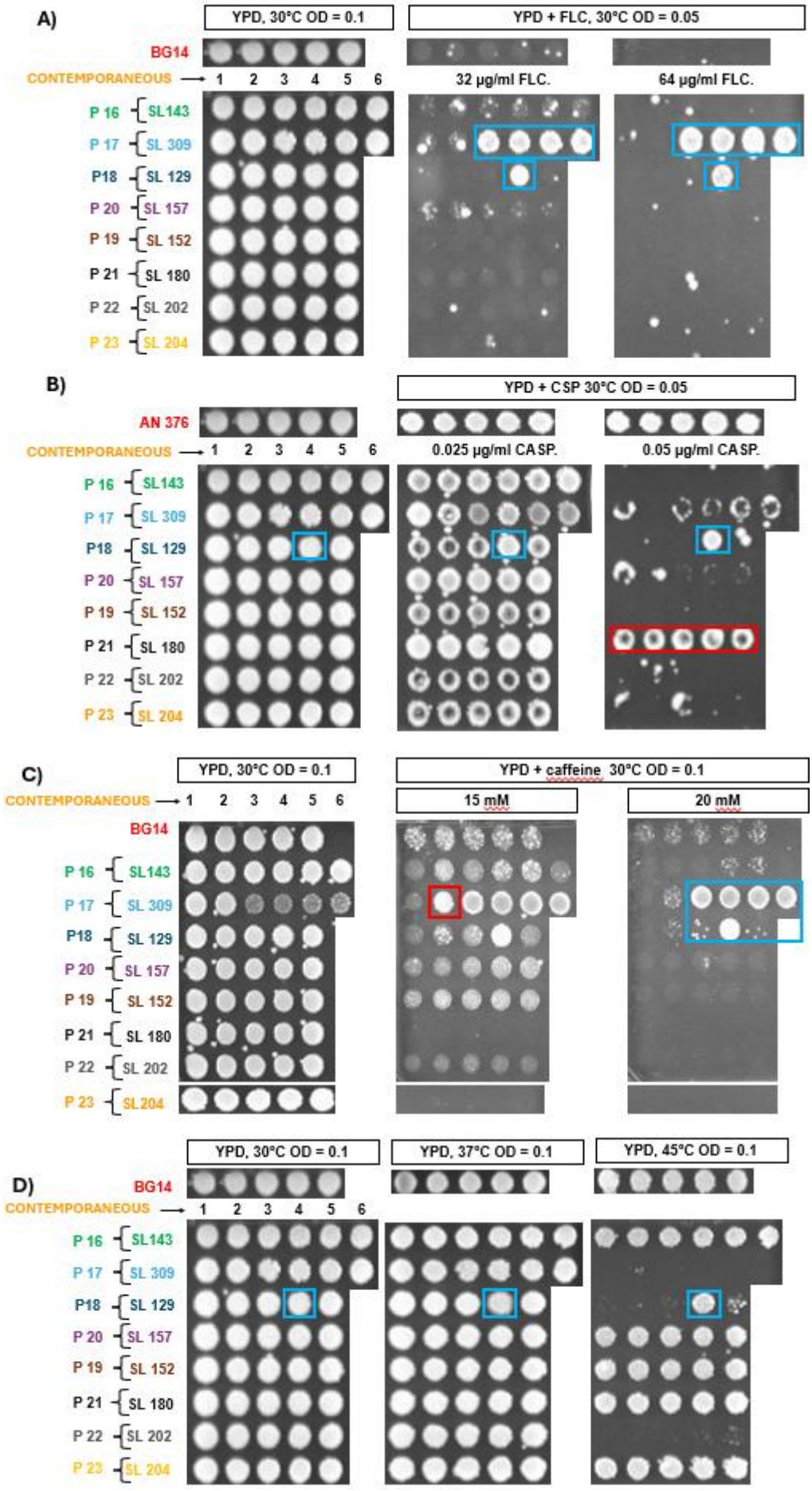
A)
YPD, 30°C OD = 0.1
YPD + FLC, 30°C OD = 0.05
BG14
CONTEMPORANEOUS → 1 2 3 4 5 6
32 µg/ml FLC.
64 µg/ml FLC.
P 16 SL143
P 17 SL 309
P18 SL 129
P 20 SL 157
P 19 SL 152
P 21 SL 180
P 22 SL 202
P 23 SL 204
B)
YPD + CSP 30°C OD = 0.05
AN 376
CONTEMPORANEOUS → 1 2 3 4 5 6
0.025 µg/ml CASP.
0.05 µg/ml CASP.
P 16 SL143
P 17 SL 309
P18 SL 129
P 20 SL 157
P 19 SL 152
P 21 SL 180
P 22 SL 202
P 23 SL 204
C)
YPD, 30°C OD = 0.1
YPD + caffeine 30°C OD = 0.1
CONTEMPORANEOUS → 1 2 3 4 5 6
15 mM
20 mM
BG14
P 16 SL143
P 17 SL 309
P18 SL 129
P 20 SL 157
P 19 SL 152
P 21 SL 180
P 22 SL 202
P 23 SL204
D)
YPD, 30°C OD = 0.1
YPD, 37°C OD = 0.1
YPD, 45°C OD = 0.1
BG14
CONTEMPORANEOUS → 1 2 3 4 5 6
P 16 SL143
P 17 SL 309
P18 SL 129
P 20 SL 157
P 19 SL 152
P 21 SL 180
P 22 SL 202
P 23 SL 204

Supplementary Fig. S5. **Susceptibility assays of contemporaneous strains from urine cultures by drop-spot assay.**

C. glabrata contemporaneous strains were adjusted at OD_{600} = 0.1 or 0.05 and then spotted on YPD plates at different concentrations of FLC (8, 16, 32, and 64 µg/mL), CSP (0.0125, 0.025, and 0.05 µg/mL), temperatures (30, 37, 44, and 45°C), and H_2O_2 (5, 10, and 15 mM). **A)** Four strains from P17 and one from P18 are FLC^R to 64 µg/mL, whereas their contemporaneous strains are susceptible at this concentration. **B)** One strain from P18 is resistant to CSP at 0.05 µg/mL. In addition, all the contemporaneous strains from P21 are resistant to CSP at the same concentration. **C)** The FLC^R strains also show resistance to caffeine at 20 mM (yellow square). In addition, the second strain from P17 shows resistance to 15 mM, however, this strain is susceptible to 20 mM of caffeine (red square). The contemporaneous strains belonging to the other patients are resistant to 15 mM of caffeine, except those strains from P21 and P23. **D)** The strains from P16, 19, 20, 21, and 23 show resistance at 45°C. Only one contemporaneous strain from P18 is only resistant to 45°C.

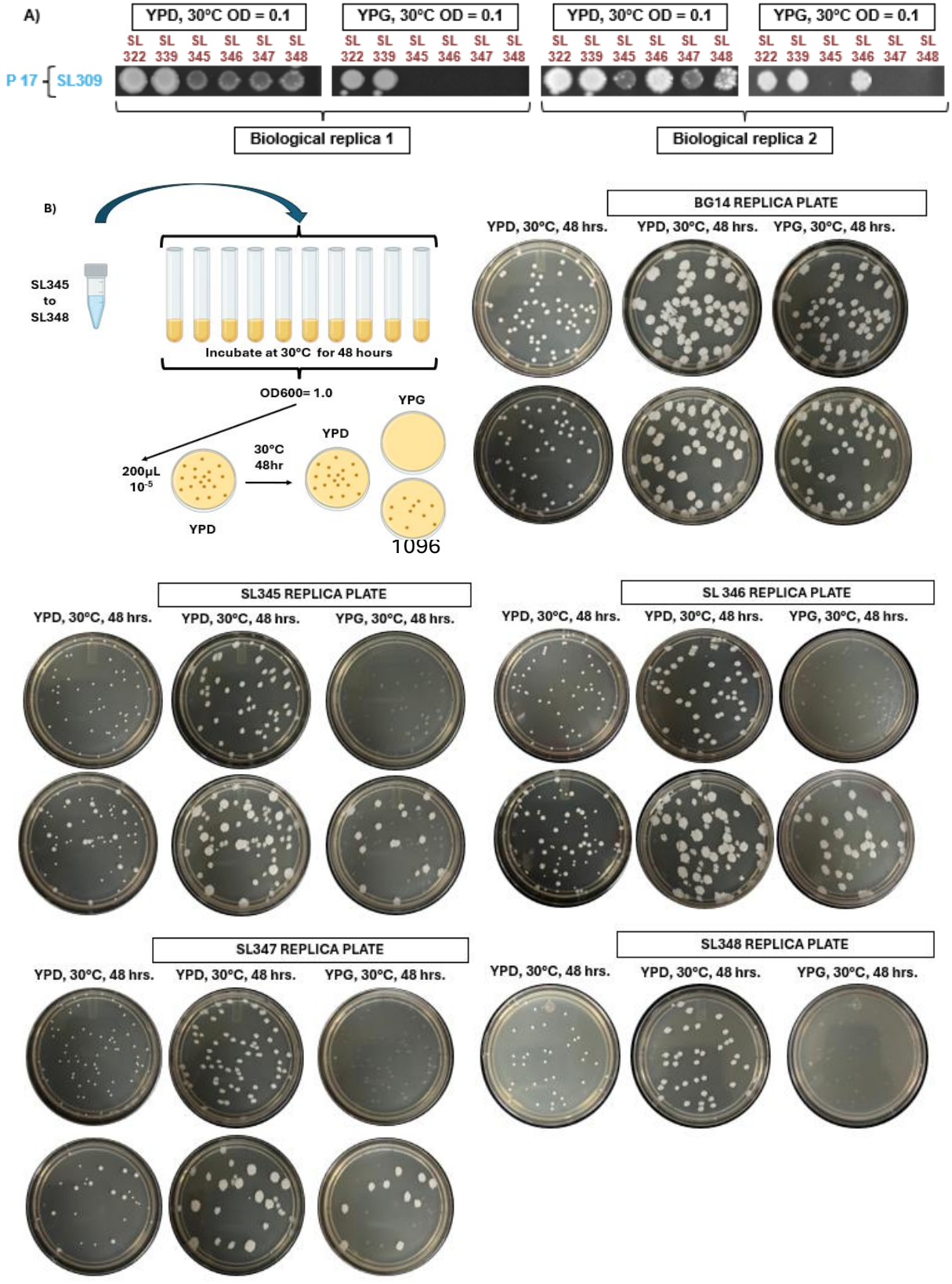
A)
YPD, 30°C OD = 0.1
YPG, 30°C OD = 0.1
YPD, 30°C OD = 0.1
YPG, 30°C OD = 0.1
SL 322 SL 339 SL 345 SL 346 SL 347 SL 348
P 17
SL309
Biological replica 1
Biological replica 2
B)
SL345 to SL348
Incubate at 30°C for 48 hours
OD600= 1.0
200µL 10-5
YPD
30°C 48hr
YPD
YPG
YPD
BG14 REPLICA PLATE
YPD, 30°C, 48 hrs.
YPD, 30°C, 48 hrs.
YPG, 30°C, 48 hrs.
SL345 REPLICA PLATE
SL 346 REPLICA PLATE
SL347 REPLICA PLATE
SL348 REPLICA PLATE

1096

Supplementary Fig. S6. Independent cultures of P17-derived strains SL345, SL346, SL347, SL348, and the ability to utilize glycerol as a carbon source. A) *C. glabrata* contemporaneous strains were adjusted at OD_{600} = 0.1 and then spotted on YPD and YPG plates. In biological replica 1, the four petite strains displayed slow growth in YPD compared with their contemporaneous strains SL322 and SL339. They also were Gly-. Nevertheless, in biological replica 2, SL346 grew well on YPG plates. **B)** The four initially classified as petite P17-derived strains were inoculated in ten independent tubes with YPD broth for 48 hours at 30°C. The OD_{600} was adjusted to 1.0, and serial dilutions were made up to 10^{-5}, 200 µL were inoculated on YPD plates, and after 48 hours replica-plated on YPD and YPG. For SL345, SL346 and SL347 small and normal colonies grew on YPD plates, but only the NCVs could grow on YPG but not the SCVs present on the same plate. SL348 did not show any normal colony.

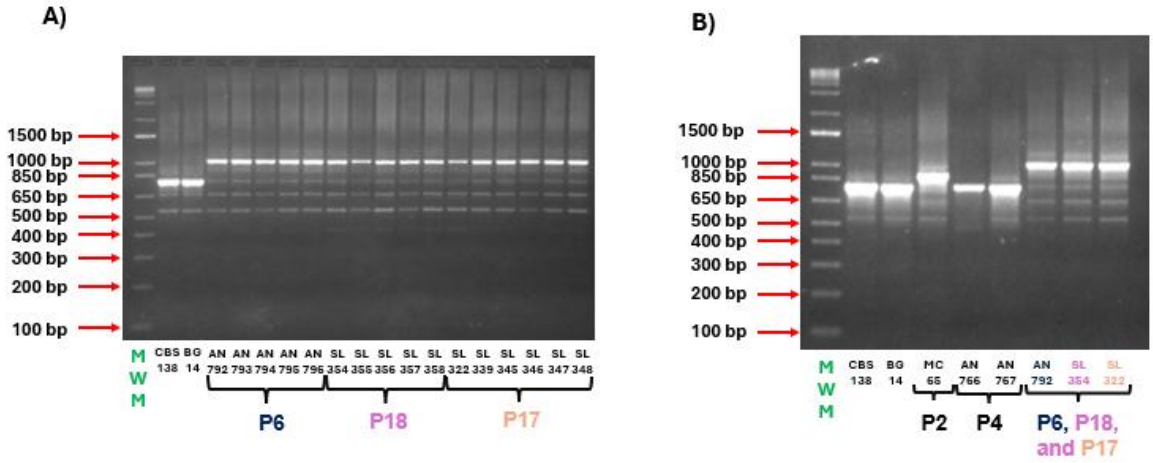

Supplementary Fig. S7. Microsatellites *EPA1* gene amplification in contemporaneous strains from P6, P17, and P18.

C*. glabrata* contains a repeated tandem sequence rich in S-T amino acids formed by 40 amino acids (120 nucleotides), and these can vary in length among strains. gDNA was used to amplify these microsatellites in contemporaneous strains. **A)** P6, P17, and P18 contemporaneous strains displayed the same PCR product sizes, but they were different from reference strains CBS138 and BG14. **B)** Comparison of a representative contemporaneous strain from P6, P17, and P18 with other strains derived from different patients from the laboratory collection. Strains derived from P6, P17, and P18 differed from those from P2, P4, and the reference strains.

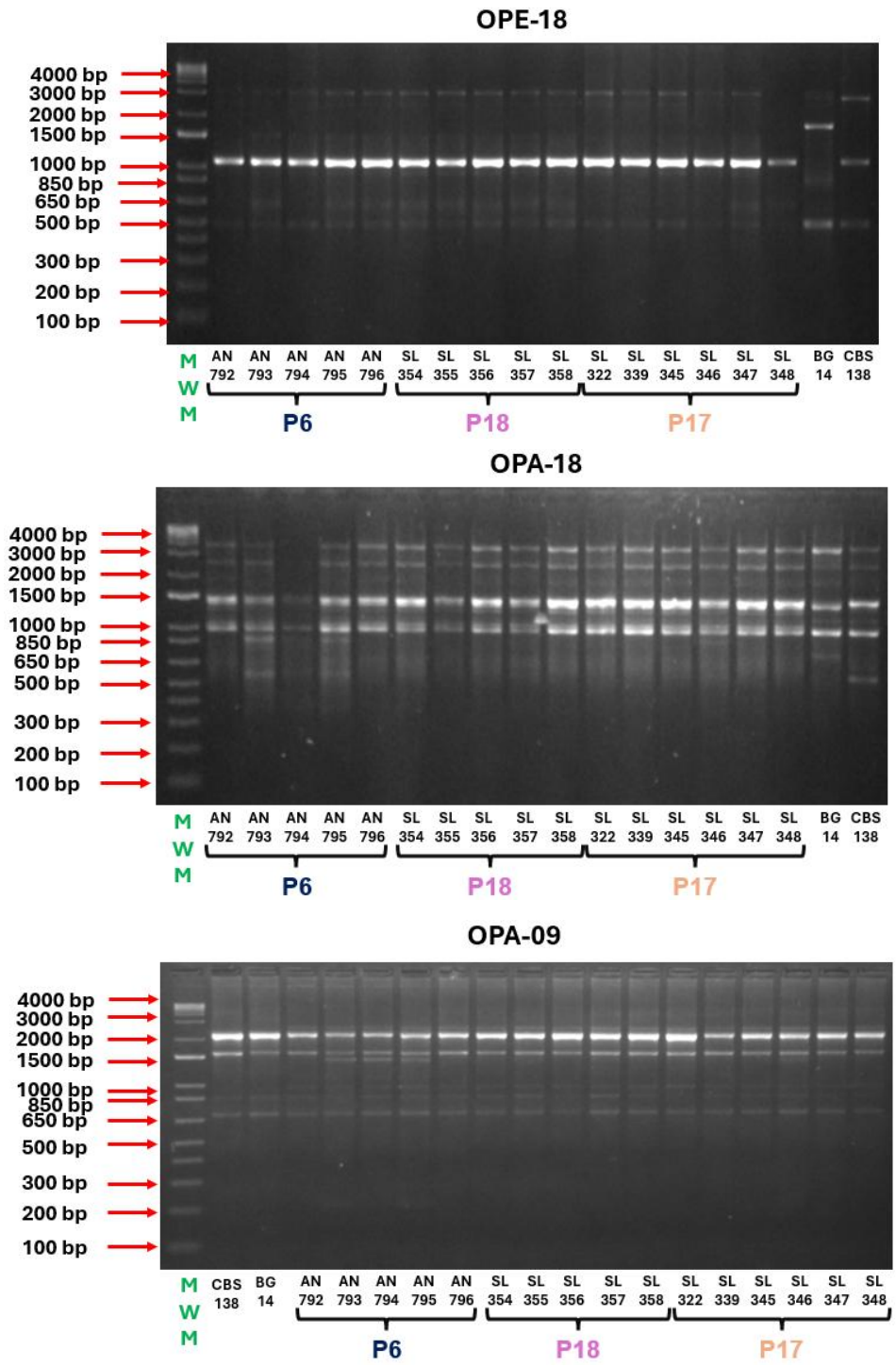

Supplementary Fig. S8. Band patterns and dendrogram of the RAPD method from contemporaneous strains from P6, P17, and P18

OPE-18, OPA-18, and OPA-09 single primers are used to amplify random fragments in the genome of *C. glabrata*. Pattern bands for each contemporaneous strain from

P6, P17, and P18 were the same, but only in OPE-18 did reference strains show differences compared to contemporaneous strains.

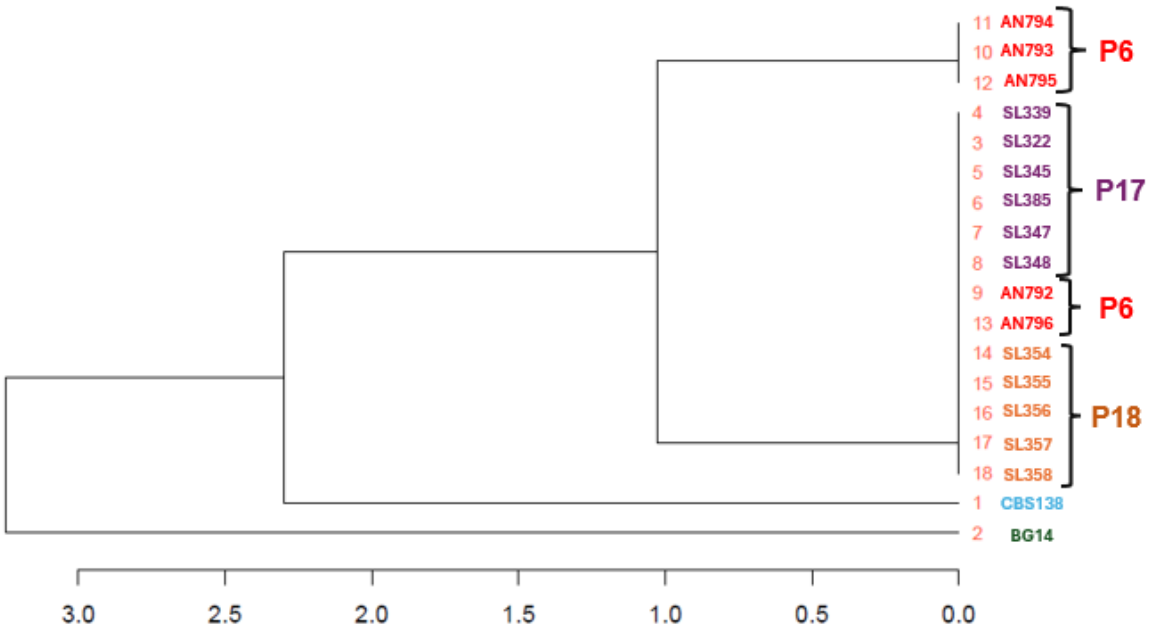

Supplementary Fig. S9. Dendrogram of *C. glabrata* contemporaneous strains from P6, P17, and P18 by RAPD method.

ImageJ® and RStudio® were used to construct a dendrogram based on the patterns of PCR products obtained using OPE-18, OPA-18, and OPA-09 primers from strains of P6, P17, and P18. The contemporaneous strains likely share a clonal origin with their patients because they were clustered together and separately from the reference strains, but they share the same phylogenetic clade. However, AN793, AN794, and AN795 from P6 are separate from other contemporaneous strains but are clustered in the same genotype.